A STUDY OF THE CAPTURE COEFFICIENTS OF NITROGEN ANS CARBON DIOXIDE

by

Donald Roger Breckenridge

UNITED STATES
NAVAL POSTGRADUATE SCHOOL

THESIS

A STUDY OF THE CAPTURE COEFFICIENTS

OF NITROGEN AND CARBON DIOXIDE

by

Donald Roger Breckenridge

June 1968

A STUDY OF THE CAPTURE COEFFICIENTS OF NITROGEN AND CARBON DIOXIDE

by

Donald Roger Breckenridge
Lieutenant, United States Navy
B. S., University of South Carolina, 1960

Submitted in partial fulfillment of the
requirements for the degree of

MASTER OF SCIENCE IN MECHANICAL ENGINEERING

from the

NAVAL POSTGRADUATE SCHOOL
June 1968

ABSTRACT

The capture coefficients were determined for carbon dioxide, nitrogen, and argon on a flat cryopanel. The gas flow rates studied varied between 0.021 torr liters per second and 0.433 torr liters per second. For flow rates greater than 0.05 torr liters per second the capture coefficients for each of the gases decreased with an increasing flow rate. It was found that the capture coefficients of carbon dioxide also depend upon the cryopanel temperature. Above 0.05 torr liters per second the capture coefficients decreased with an increasing cryopanel temperature.

TABLE OF CONTENTS

Section	Title	Page
1.	Introduction	13
2.	Cryopumping	14
3.	The Capture Coefficient	17
3.1	Theoretical Development of the Capture Coefficient	17
3.2	Relationship Between the Capture Coefficient and the Condensation Coefficient	19
4.	Experimental Determination of the Capture Coefficient	23
4.1	Experimental Technique	23
4.2	Experimental Equations	24
4.3	Experimental Measurements	26
5.	Discussion of Results	29
5.1	Experimental Results	29
5.2	Comparison with Published Data	37
6.	Uncertainty Analysis	41
7.	Conclusion	43
	Bibliography	45
Appendix A	General Description of the Systems	47
Appendix B	Cryogenic Transfer System	52
Appendix C	Gas Addition and Flow Measurement System	54
Appendix D	Operating Procedures	56
Appendix E	Model Analysis of ΔP	60
Appendix F	Computer Program for Data Reduction	74

LIST OF TABLES

Table		Page
I	Experimental Data for Cryopumping Carbon Dioxide	31
II	Experimental Data for Cryopumping Nitrogen	33
III	Experimental Data for Cryopumping Argon	35
IV	Typical Reported Capture Coefficients of Carbon Dioxide	38
V	Typical Reported Capture Coefficients of Nitrogen	39
VI	Typical Reported Capture Coefficients of Argon	40
VII	Uncertainties in Measured Values	42
VIII	Coefficients of System Equations	68

LIST OF ILLUSTRATIONS

Figure		Page
1.	Vapor Pressure of Various Gases	16
2.	Pressure vs Time for Condensable Gas Only	24
3.	Pressure vs Time Condensable and Noncondensable Gases Present	27
4.	Capture Coefficient vs Flow Rate for Carbon Dioxide	32
5.	Capture Coefficient vs Flow Rate for Nitrogen	34
6.	Capture Coefficient vs Flow Rate for Argon	36
7.	Flow Regimes	44
8.	Schematic of the System	49
9.	Cryopanel	50
10.	Location of Thermocouples	51
11.	Schematic of Cryogenic Fluid Transfer System	53
12.	Gas Addition and Flow Measurement System	55
13.	Model for Analysis of Pressure Drop	62
14.	Diffusion Pump Characteristics	65
15.	Conductance Effects	72

LIST OF SYMBOLS

A	surface area	cm^2
A_s	cryosurface area	cm^2
f	capture coefficient	
f^*	capture coefficient measured without conductance	
f_g	condensation coefficient	
f_s	evaporation coefficient	
k	Boltzmann constant	erg $°K^{-1}$
M	molecular weight	gm $(gm.mole)^{-1}$
m	mass of a molecule	gm
n	number of molecules per unit volume	cm^{-3}
N	total number of molecules	
N_A	Avogadro's number	
$\dot{N}$	number of molecules per unit time	sec^{-1}
$\dot{N}_a$	summation of molecular flow into V_a	sec^{-1}
$\dot{N}_{ai}$	flow of molecules from V_a to V_i	sec^{-1}
$\dot{N}_D$	flow of molecules to diffusion pump	sec^{-1}
$\dot{N}_i$	summation of molecular flow into V_i	sec^{-1}
$\dot{N}_{io}$	flow of molecules from V_i to V_o	sec^{-1}
$\dot{N}_L$	flow of molecules into V_a from gas addition system	sec^{-1}
$\dot{N}_o$	summation of molecular flow into V_o	sec^{-1}
$\dot{N}_r$	flow of residual gas molecules	sec^{-1}
P	total pressure	torr
$\dot{P}$	pressure per unit time	torr sec^{-1}
P_e	chamber equilibrium pressure with gas flow on	torr
P_g	chamber equilibrium pressure with no gas flow	torr
P_i	pressure in V_i	torr

P_L	pressure at entrance to V_a	torr
P_o	pressure in V_o	torr
P_t	transition pressure	torr
Q_L	throughput rate	torr liter sec^{-1}
R	universal gas constant	$erg°K^{-1}gm\text{-}mole^{-1}$
S_{th}	theroretical specific pumping speed	liter $sec^{-1}cm^{-2}$
T	absolute temperature	°K
T_a	temperature in V_a	°K
T_g	gas temperature	°K
T_i	temperature in V_i	°K
T_L	temperature in V_L	°K
T_o	temperature in V_o	°K
T_s	temperature of the cryosurface	°K
V	volume	cm^3
$\dot{V}$	volume per unit time	cm^3sec^{-1}
$\dot{V}_{th}$	theoretical pumping speed	cm^3sec^{-1}
$\dot{V}_{exp}$	experimental pumping speed	cm^3sec^{-1}
V_a	volume of gas addition piping	cm^3
$\dot{V}_D$	diffusion pump volumetric flow rate	cm^3sec^{-1}
V_i	volume within the radiation shielding	cm^3
V_L	volume of auxiliary vacuum system	cm^3
V_o	volume between shielding and chamber walls	cm^3
α	diffusion pump efficiency factor	
β	conductance area between V_o and V_i	cm^2
ΔP_m	$(P_e - P_g)$ measured	torr
μ	micron	
γ	correction factor	

ACKNOWLEDGEMENTS

The work described herein was made possible by the continued support of the Office of Naval Research through the Foundation Research Program.

The author wishes to express his gratitude to Dr. Paul F. Pucci for his continued support and encouragement. He also wishes to thank Mr. K. Smith for his valuable technical assistance. Last but not least he wishes to thank his wife, Bobbi, for her understanding during the course of this work.

1. Introduction.

Since the advent of the space age it has become more and more important to be able to simulate outer space conditions for testing purposes. It has been proven that the cryopump provides the high pumping speeds necessary to handle large gas loads such as test firing rockets. The cryopump is not the ultimate pumping process but is an important part of an overall pumping system which may include mechanical, diffusion, and adsorption systems.

To properly design a cryopump the capture coefficients of the gases to be pumped must be known. It is the purpose of this work to study the capture coefficients of carbon dioxide, nitrogen, and argon. The intention is to show that the capture coefficients are dependent upon the gas flow rate into the system and also the cryopump temperature.

2. Cryopumping.

Cryopumping is a process by which a high vacuum can be maintained in a system by freezing the gas molecules on a cryogenically cooled surface. The cryopump may be of any configuration. In the present case it is a flat panel embossed on one side to allow for the passage of a cryogenic fluid.

The advantages of the cryopump are many. For example, for testing space vehicles the cryopump provides a high specific pumping speed. In addition, the size of the cryopump is small for a given pumping speed versus a diffusion pump. Other advantages include: the pumping surface can be placed directly in the chamber to be evacuated; the cryopump can be made in almost any configuration; and there is no pumping fluid exposed to the high vacuum chamber. In the space simulation field the low temperatures required for cryogenic pumping are also required for temperature simulation (1).

Certain disadvantages are inherent in the system. The vapor pressure of a solidified gas can be represented by an equation of the form

$$\text{Log}_{10} P = A - \frac{B}{T} \qquad (2.1)$$

Where T is the absolute temperature and A and B are constants. Figure 1 is a plot of Vapor Pressure versus the reciprocal of Absolute Temperature. It can be seen that certain gases cannot be pumped using a cryopump if the cryopanel is at 20°K, namely neon, hydrogen, and helium (which is so high it is not shown in Figure 1). If the cryopanel is above 20°K the freezing temperature of other gases may be below the cryopanel temperature and will remain in the gaseous phase. In this connection it is necessary to include additional pumps in the system. That is, diffusion pumps backed by

mechanical pumps will be required to reduce the amount of noncondensables.

Another disadvantage of a cryopump is the buildup of condensate on its surface. When the layer becomes too thick the panel must be warmed up in order to eliminate the buildup.

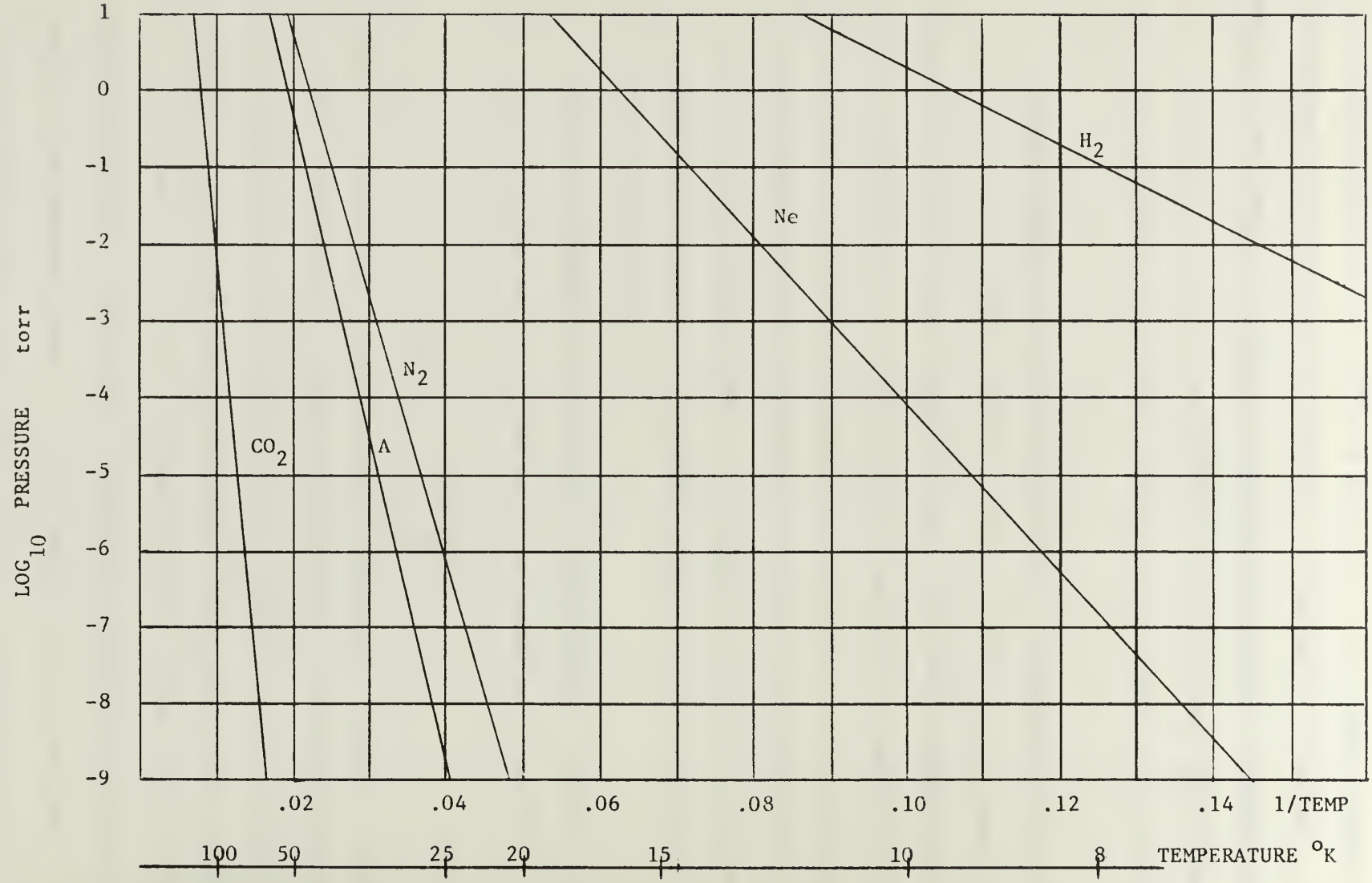

FIGURE 1. VAPOR PRESSURE OF VARIOUS GASES

3. The Capture Coefficient.

3.1 Theoretical Development of the Capture Coefficient.

The following development of the capture coefficient is general and follows closely that of Haygood and Dawson (2).

The capture coefficient is defined as the ratio of the actual number of molecules captured by a cold surface to the theoretical maximum number that could be captured. The actual volumetric rate of molecules captured by the cryopanel is now defined as the experimental pumping speed $\dot{V}_{exp}$. In the same manner the theoretical maximum volumetric rate of molecules that could be captured is defined as the theoretical pumping speed $\dot{V}_{th}$. The capture coefficient f is then:

$$f = \frac{\dot{V}_{exp}}{\dot{V}_{th}} \tag{3.1}$$

a. Theoretical Pumping Speed

In a high vacuum the gas molecules collide with the walls more frequently than with other molecules. This is called the free molecular region. In the free molecular region the theoretical pumping speed may be derived using the kinetic theory of gases.

The ideal gas law states:

$$PV = NkT \tag{3.2}$$

where P = chamber pressure, torrs

V = chamber volume, cm^3

N = total number of molecules

k = Boltzmann constant, erg/°K

T = absolute temperature, °K

Taking the derivative with respect to time leads to:

$$\dot{V} = \frac{kT}{P}\dot{N} \tag{3.3}$$

since we are interested in what happens at a specific pressure and temperature.

Kinetic theory defines pressure as,

$$P = \frac{\dot{N}}{A} [2\pi m k T]^{\frac{1}{2}} \tag{3.4}$$

where

$\dot{N}$ = number of molecules per unit time, sec^{-1}

A = surface area, cm^2

m = mass of one molecule, grams

Substituting equation 3.4 into 3.3 produces,

$$\dot{V} = A \left[\frac{kT}{2\pi m} \right]^{\frac{1}{2}} \tag{3.5}$$

Since $k = \frac{R}{N_A}$ and $m = \frac{M}{N_A}$,

where

R = universal gas constant, erg/gm - mole °K

N_A = Avogadro's number, $(gm - mole)^{-1}$

M = molecular weight, gm/gm-mole

equation 3.5 becomes

$$\dot{V}_{th} = A_s \left[\frac{R T_g}{2\pi M} \right]^{\frac{1}{2}} \tag{3.6}$$

where

$\dot{V}_{th}$ = theoretical pumping speed, cm^3/sec

A_s = area of cryopanel surface, cm^2

T_g = temperature of gas, °K

b. Experimental Pumping Speed.

When a gas load is applied through a controlled leak to the chamber we arrive at the following continuity equation.

$$\frac{P\dot{V}_L}{RT_L} = \frac{P\dot{V}}{RT_g} + \frac{V\dot{P}}{RT_g} \tag{3.7}$$

where the subscript "L" refers to the controlled leak and the subscript "g" to the gas. The left-hand side of the equation represents the rate of flow of gas into the system and the right-hand side the total number of moles of gas condensed per second. If the chamber reaches an equilibrium pressure P_e, then $\dot{P}$ is zero and

$$\frac{P\dot{V}_L}{RT_L} = \frac{P_e\dot{V}}{RT_g} \tag{3.8}$$

Define the gas throughput Q_L as:

$$Q_L = P_L\dot{V}_L \tag{3.9}$$

then from equation (3.8)

$$\dot{V}_{exp} = \frac{Q_L T_g}{P_e T_L} \tag{3.10}$$

c. Capture Coefficient.

From equations (3.1), (3.6), and (3.10)

$$f = \frac{Q_L T_g}{P_e T_L}\,\frac{1}{A_s}\left[\frac{2\pi M}{RT_g}\right]^{\frac{1}{2}} \tag{3.11}$$

3.2 Relationship Between the Capture Coefficient and the Condensation Coefficient.

To assist in the determination of the capture coefficient it is advantageous to relate it to the condensation coefficient.

On a macroscopic scale classical condensation - evaporation theory may be utilized in an attempt to understand the solid-gas interface phenomenon. Consider the case of a pure condensed gas in an isothermal enclosure. The vapor and solid phases will be in equilibrium at a pressure equal to the vapor pressure. The number of vapor molecules

incident on the solid per unit time is given by equation (3.4).

$$\dot{N} = \frac{P_v A}{[2\pi m k T]^{\frac{1}{2}}} \tag{3.4}$$

where the subscript "v" refers to vapor. Of these incident molecules, a certain fraction f will condense and a fraction (1-f) will be reflected. In addition a certain number of molecules will evaporate. At equilibrium, the number of molecules that evaporate must equal the number condensing. The fraction f is then the isothermal equilibrium condensation coefficient. Since the vapor is in equilibrium with the condensate, the number of molecules condensed will be equal to the number which evaporated and there will be no net transfer of mass or energy. Hence,

$$\left[\frac{f P_v}{\sqrt{T}}\right]_{COND} = \left[\frac{f P_v}{\sqrt{T}}\right]_{EVAP} \tag{3.12}$$

In the present case a temperature difference exists between the gas and solid phases. The rate of condensation of the gas is

$$\dot{N}_{COND} = \frac{f_g P_g A}{[2\pi m k T_g]^{\frac{1}{2}}} \tag{3.13}$$

where, f_g = condensation coefficient. The rate of evaporation of the solid phase is

$$\dot{N}_{EVAP} = \frac{f_s P_s A}{[2\pi m k T_s]^{\frac{1}{2}}} \tag{3.14}$$

where, f_s = evaporation coefficient and where the subscripts "g" and "s" refer to the gas and solid phases respectively. At equilibrium condition, from equations (3.13) and (3.14)

$$\frac{f_g P_g}{\sqrt{T_g}} = \frac{f_s P_s}{\sqrt{T_s}} \tag{3.15}$$

where there will be a net transfer of energy but no net mass transfer.

In addition to a temperature difference in the experimental apparatus

there will also be a transient condition. This occurs when gas is admitted to the system while the cryopanel is pumping. After a period of time the chamber will reach an equilibrium pressure P_e. At this point the actual capture rate of molecules is the difference between the condensation and evaporation rates. From equations (3.13) and (3.14)

$$\dot{N}_{acr} = \frac{f_g P_e A}{[2\pi m k T_g]^{\frac{1}{2}}} - \frac{f_s P_s A}{[2\pi m k T_s]^{\frac{1}{2}}} \tag{3.16}$$

The theoretical incidence rate of molecules on the cold surface is given by equation (3.4).

$$\dot{N}_{th} = \frac{P_e A}{[2\pi m k T_g]^{\frac{1}{2}}} \tag{3.4}$$

It will be recalled that the capture coefficient was defined as the actual volumetric rate of molecules captured to the maximum volumetric rate that could be captured. Therefore from equations (3.16) and (3.4)

$$f = f_g \left[1 - \frac{f_s P_s \sqrt{T_g}}{f_g P_e \sqrt{T_s}} \right] \tag{3.17}$$

From equation (3.15)

$$\frac{f_s}{f_g} = \frac{P_g \sqrt{T_s}}{P_s \sqrt{T_g}} \tag{3.18}$$

Which leads to

$$f = f_g \left[1 - \frac{P_g}{P_e} \right] \tag{3.19}$$

Solving equation (3.19) for f_g and substituting equation (3.11) for f yields

$$f_g = \frac{Q_L T_g}{(P_e - P_g) A_s T_L} \left[\frac{2\pi M}{R T_g} \right]^{\frac{1}{2}} \tag{3.20}$$

or

$$f_g = \frac{Q_L}{(P_e - P_g) A_s T_L} \left[\frac{2\pi M T_g}{R} \right]^{\frac{1}{2}} \tag{3.21}$$

where

f_g = condensation coefficient

Q_L = gas throughput, torr-liters/sec

P_e = equilibrium pressure with gas flow, torr

P_g = equilibrium pressure with no gas flow, torr

A_s = area of cryopanel surface, cm^2

T_L = gas temperature at leak, °K

T_g = chamber gas temperature, °K

4. Experimental Determination of the Capture Coefficient.

4.1 Experimental Technique.

A description of the system and the operating procedures are included in Appendices A, B, C, and D. In general the system consists of a stainless steel tank containing radiation shielding and the cryopanel (See Figure [8], Appendix A). Evacuation of the chamber is accomplished with a diffusion pump backed by a large mechanical forepump. The chamber is isolated from the pumps by a high vacuum gate valve. Gas is admitted to the system through a variable leak valve and a quick-acting test gas valve. The gas line has an optical baffle inside the chamber to prevent the gas from going directly to the cryopanel.

Prior to each experiment the system was pumped to base pressure on the order of 2×10^{-7} torrs. The cryopanel was then cooled, which further reduced the pressure to approximately 1.5×10^{-8} torr.

The variable leak valve was then set and the gas throughput Q_L was determined as described in Appendix C.

The experimental technique utilized to determine the capture coefficient is as follows:

1. Degas the ionization gage and zero adjust. Record the base pressure (on the order of 1.5×10^{-8} torr).

2. Admit the gas to the system continuously and record the pressure on a Mosely X-Y Plotter.

3. Isolate the system from the diffusion and mechanical pumps.

4. After three minutes close the test gas quick-acting valve.

5. Degas and zero adjust the ionization gage. Check to see that the base pressure is the same as determined in step (1).

6. Repeat the above procedure (except step 3, as the system remains in isolation) until all transients have subsided. Total gas flow

time was usually fifteen to twenty minutes.

7. Temperature readings were taken and recorded at given intervals on all thermocouples. (See Figure 10, Appendix A.)

The above technique provided the following information: the pressure drop in the chamber; the temperature of the cryopanel, gas in the chamber, and gas at the leak; and the gas throughput.

Figure 2 represents the plot of chamber pressure versus time if only condensable gases were present.

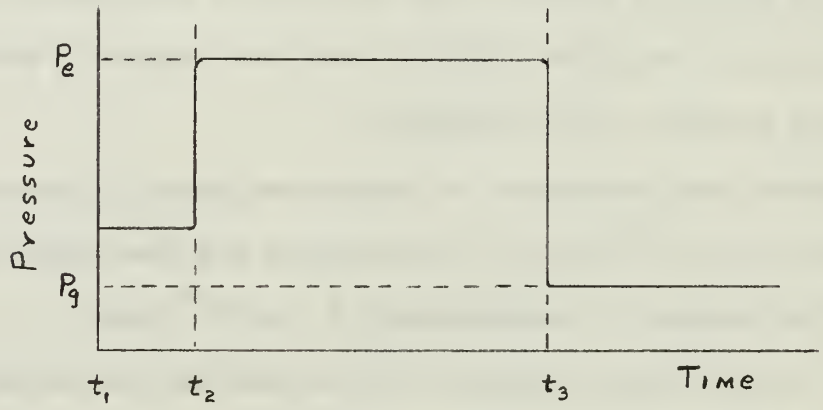

Fig. 2. Pressure vs Time for Condensable Gas Only

At time t_1, the controlled leak is open to the chamber and the system is at equilibrium with the diffusion pump and the cryopanel. At time t_2 the system is isolated from the diffusion pump and comes to a new equilibrium pressure P_e. At time t_3 the test gas quick-acting valve is closed and the pressure drops to the base pressure P_g.

4.2 Experimental Equations.

The following expression for the condensation coefficient was arrived at in equation (3.21).

$$f_g = \frac{Q_L}{(P_e - P_g) A_s T_L} \left[\frac{2\pi M T_g}{R}\right]^{\frac{1}{2}} \qquad (4.1)$$

The capture coefficient may then be determined from equation (3.19).

$$f = f_g \left[1 - \frac{P_g}{P_e} \right] \tag{4.2}$$

It can be seen that when $P_e >> P_g$ the capture coefficient is equal to the condensation coefficient.

A Bayard-Alpert ionization gage was used to measure pressures in the chamber. These ionization gages are calibrated at the factory with nitrogen at ambient room temperature. When gas pressures other than nitrogen are measured a gage factor must be applied. Letting $\Delta P_m = P_e - P_g$, then $\Delta P_{act} = (G.F.) \Delta P_m$ where the subscript "m" indicates the measured pressure. Equation (4.1) then becomes

$$f_g = \frac{Q_L}{\Delta P (G.F.) A_s T_L} \left[\frac{2\pi M T_g}{R} \right]^{\frac{1}{2}} \tag{4.3}$$

The pressure measurements were made with the ionization gage located at the chamber wall. The chamber wall was at ambient room temperature, therefore, thermal transpiration effects were not present. However, since the gage was located outside of the radiation shield the conductance effect must be included in the calculations.

The relationship between the capture coefficient and conductance area is derived in Appendix E. Equation (E.41) becomes

$$f^* = \frac{1}{\frac{1}{f} + \frac{A}{\beta}} \tag{4.4}$$

where f* = capture coefficient measured without conductance

f = capture coefficient measured with conductance

β = conductance area

A = area of cryopanel

4.3 Experimental Measurements.

Examination of equation (4.3) reveals which parameters must be measured to determine the capture coefficient.

$$f_g = \frac{Q_L}{\Delta P (G.F.) A_s T_L} \left[\frac{2\pi M T_g}{R}\right]^{\frac{1}{2}} \qquad (4.3)$$

For a given gas $\frac{1}{(G.F.)A_s}\left[\frac{2\pi M}{R}\right]^{\frac{1}{2}}$ is a constant; then

$$f_g = (\text{CONSTANT})\ \frac{Q_L \sqrt{T_g}}{\Delta P\ T_L} \qquad (4.5)$$

a. Throughput at the Controlled Leak.

The flow rate Q_L was calculated by measuring the rate of pressure rise in a known volume. The system is shown in Figure 12, Appendix C. The experimental procedure is outlined in Appendix C and the flow rate calculated from equation (C.1.)

$$Q_L = \dot{P} V \qquad (C.1)$$

where

Q_L = flow rate, torr liters/sec

$\dot{P}$ = rate of pressure rise in the auxiliary volume, torr/sec.

V = auxiliary volume, liters

b. Pressure Drop Measurement.

The pressure drop ΔP was measured utilizing a Bayard-Alpert ionization gage mounted on the chamber wall. A cold cathode trigger gage was mounted on the opposite side and was used as a check. A complete analysis of the pressure drop method is included in Appendix E.

In section 4.1 it was assumed that only condensable gases were present in the system. When carbon dioxide was admitted to the system and the cryopanel was at 88°K the experimental technique was modified due

to the presence of noncondensable gases. The pressure versus time curve is shown in Figure 3.

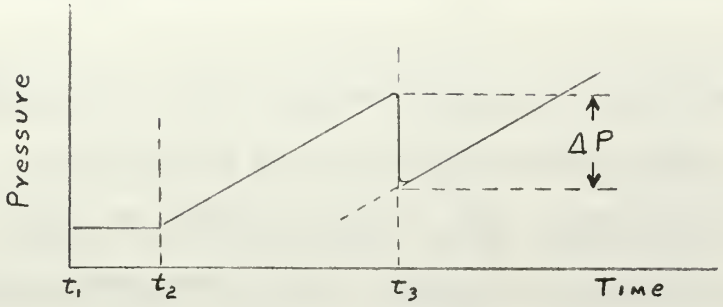

Fig. 3. Pressure vs Time Condensable and Noncondensable Gases Present

At time t_1, the controlled leak is opened to the main chamber. At time t_2 the system is isolated from the diffusion pump. At time t_3 the test gas quick-acting valve is closed. The resulting pressure drop ΔP was then measured as shown at time t_3.

In order to reduce the effects of other condensable and noncondensable gases, only high purity research gas was used. Except for carbon dioxide on an 88°K cryopanel the effect of non-condensable gases was not seen and the system base pressure P_g was constant.

An improvement in the measurement of the pressure drop could be attained if a mass spectrometer were employed. The mass spectrometer measures the partial pressure of the gas under consideration, whereas, an ionization gage only measures the total chamber pressure. This equipment was not available, therefore only the total chamber pressure was measured.

c. Gas Temperature Measurement.

In this system the ratio of the area of the radiation shields to the area of the cryopanel is large. The assumption was made that the gas struck the shields prior to striking the cryopanel and therefore assumed the temperature of the shields.

Consequently, thermocouples were installed on the shields as shown in Figure 10, Appendix A. The thermocouples were monitored to determine T_g.

A thermocouple was installed just prior to the test gas quick acting valve. This thermocouple was used to determine T_L.

All thermocouples were Teflon insulated, 24 gage copper-constantan. The temperatures were monitored with an automatic digital voltmeter-printer combination.

5. Discussion of Results.

5.1 Experimental Results.

The results of determining the capture coefficients of carbon dioxide, nitrogen and argon verified that the capture coefficient is dependent upon the flow rate of gas into the system above .05 torr-liters/sec. From the study of nitrogen and carbon dioxide there appears to be a dependence of the capture coefficient upon the cryopanel temperature. The results are presented in Figures 4, 5, and 6 and in tabular form in Tables I, II, and III.

a. Carbon Dioxide

Figure 4 is a plot of Table I. Below .05 torr liters/sec. the capture coefficient appears to converge to the same average value for cryopanel temperatures between 27°K and 84°K. As the flow rate approaches 0.25 torr-liters/sec. the separation of the temperature lines becomes apparent.

b. Nitrogen

Figure 5 is a plot of Table II. The plot is approximately ten percent below the plot obtained by Bevan (3) utilizing the same equipment in 1967. The difference is attributed to utilizing a different ionization gage. The shape of the curve is the same as Bevan's. Below .05 torr-liters/sec. the capture coefficient appears to become constant. Data was not obtained for cryopanel temperatures significantly above 30°K, however, upon stopping the refrigeration at the end of a day's run the tank pressure began to rise rapidly. This indicated that with a cryopanel temperature rise of approximately 5°K the cryopanel could no longer immobilize all of the nitrogen molecules.

c. Argon

Figure 6 is a plot of Table III. The capture coefficient of argon was much lower than expected. At flow rates above .05 torr-liters/sec., the curve shows the dependence of the capture coefficient upon the flow rate.

d. General

A comment is in order concerning the determination of the cryopanel temperature. The cryopanel was instrumented with copper-constantan thermocouples. The sensitivity of the copper-constantan thermocouples is about 40 microvolts per degree at room temperature, but only about 5 microvolts per degree at 20°K. The latter fact leads to possible errors when attempting to determine low temperatures (4).

All reported temperatures (Tables I, II, and III) below 35°K were taken when the average of the helium supply and return temperatures for the cryopanel was between 7.0°K and 8.0°K. In Table I for the reported temperatures of about 46°K, the average helium temperature was between 15.0°K and 16.0°K. The helium supply and return temperatures were taken at the helium refrigerator from two Hiese Gages.

Table I

Experimental Data for Cryopumping Carbon Dioxide

Flow $\frac{\text{torr liters}}{\text{sec}}$	ΔP_m x 10^{-6} torr	T_s °K	T_g °K	Capture Coefficient
.034	2.00	27.4	296	.557
.060	3.56	27.9	296	.559
.072	4.55	39.0	295	.534
.080	4.80	39.1	294	.559
.110	6.96	27.7	297	.533
.118	8.55	38.7	294	.481
.156	11.7	40.0	292	.469
.157	12.7	39.0	294	.440
.158	11.9	28.8	296	.464
.188	17.5	38.7	294	.392
.208	18.5	28.3	296	.408
.244	24.5	37.5	291	.368
.253	29.1	38.5	294	.327
.276	34.0	27.5	296	.307
.277	32.8	37.5	291	.320
.282	37.0	37.9	293	.292
.338	49.0	27.0	296	.270
.088	5.40	46.1	296	.545
.116	7.75	46.7	294	.512
.173	15.1	46.6	294	.412
.202	17.5	47.0	294	.415
.260	31.5	46.7	294	.312
.286	39.0	45.5	294	.281
.026	1.57	89.9	295	.548
.027	1.52	89.4	295	.589
.103	7.70	93.6	294	.467
.185	16.2	90.2	299	.411
.266	36.8	89.4	297	.278
.301	47.3	87.0	296	.247
.350	64.8	87.6	298	.214
.400	87.5	90.3	298	.184

Note: Gage Factor 0.73

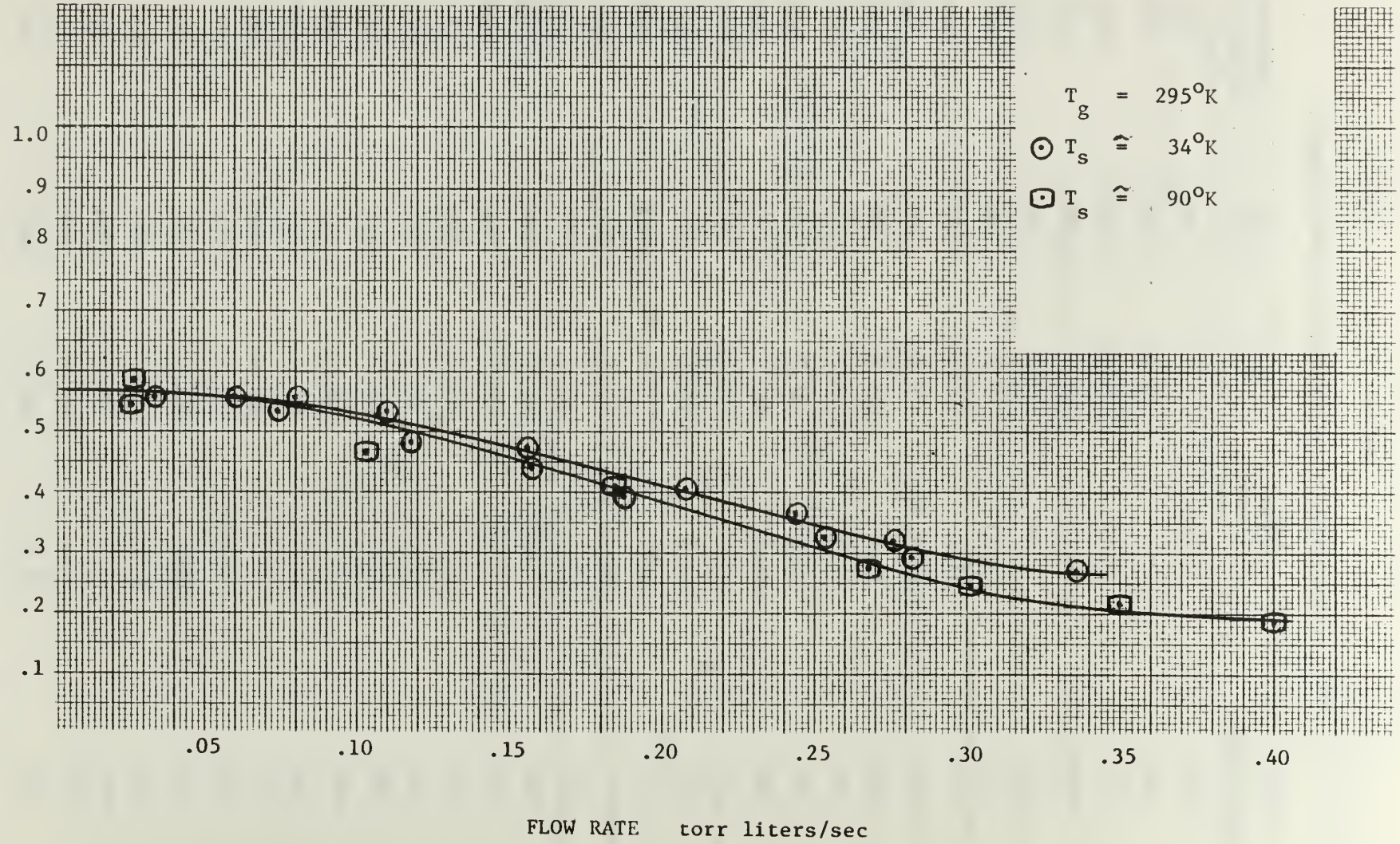

FIGURE 4. CAPTURE COEFFICIENT vs FLOW RATE FOR CARBON DIOXIDE

Table II

Experimental Data for Cryopumping Nitrogen

Flow $\frac{\text{torr liters}}{\text{sec}}$	ΔP_m x 10^{-6} torr	T_s °K	T_g °K	Capture Coefficient
.044	1.46	29.2	294	.560
.050	1.77	27.7	293	.552
.061	2.15	27.3	293	.548
.066	2.24	35.2	294	.570
.079	3.02	27.6	293	.519
.102	3.86	34.9	293	.520
.125	4.85	22.2	294	.514
.164	7.51	34.6	292	.447
.175	9.16	22.3	294	.404
.218	12.6	33.7	292	.369
.242	15.0	24.5	293	.351
.278	19.9	31.5	292	.278
.292	20.5	25.1	293	.316
.306	22.6	27.5	295	.298
.368	30.5	25.8	293	.274
.364	32.3	30.2	294	.254
.410	40.5	26.3	293	.232
.433	40.6	30.0	295	.241

Note: Gage Factor 1.00

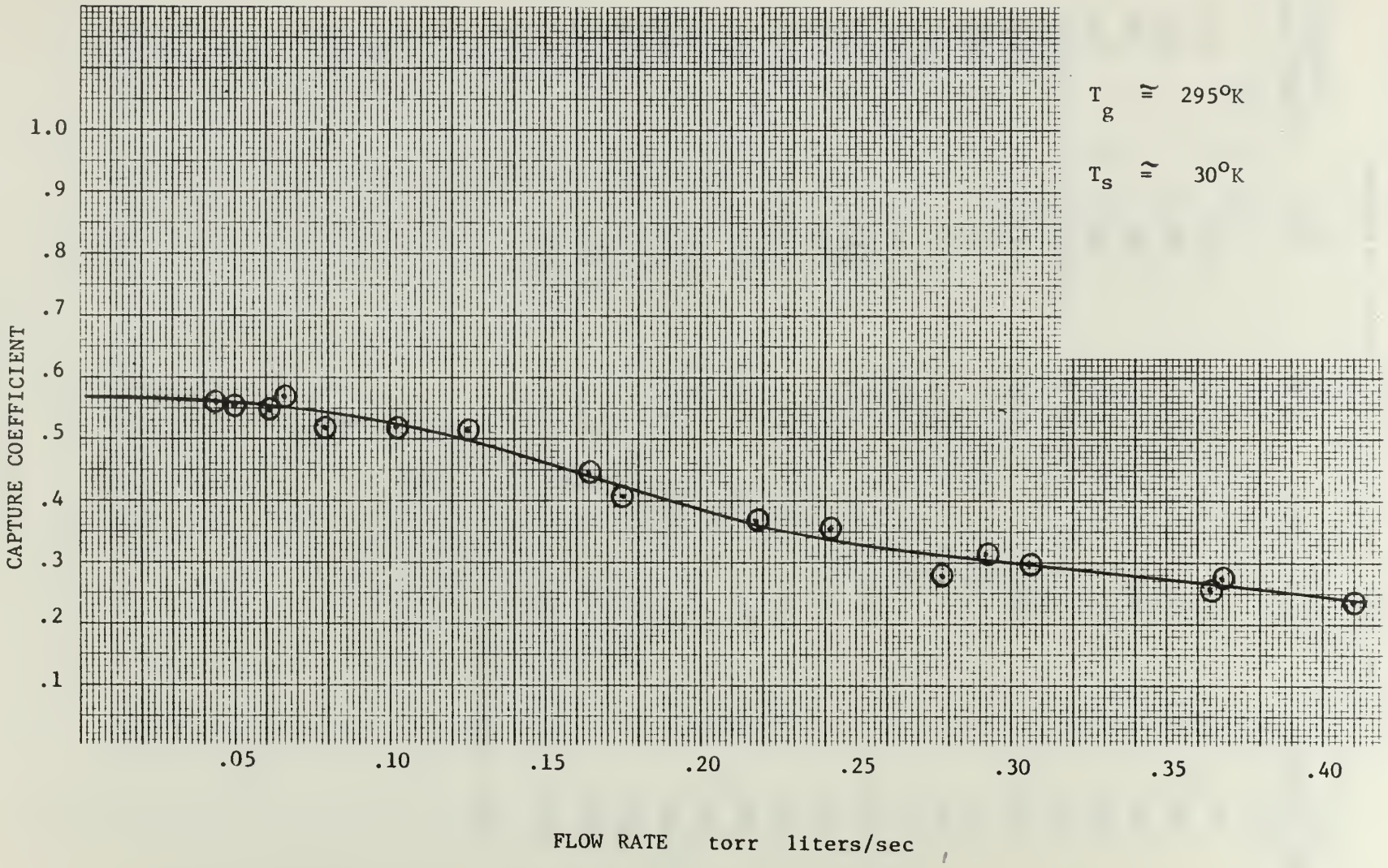

FIGURE 5. CAPTURE COEFFICIENT vs FLOW RATE FOR NITROGEN

Table III

Experimental Data for Cryopumping Argon

Flow $\frac{\text{torr liters}}{\text{sec}}$	ΔP_m x 10^{-6} torr	T_s °K	T_g °K	Capture Coefficient
.021	1.84	26.6	294	.355
.044	3.80	22.2	295	.345
.074	7.40	24.2	295	.315
.118	11.60	23.3	295	.315
.150	16.80	25.6	295	.280
.182	23.90	25.7	295	.245
.223	32.40	26.5	295	.225
.256	46.00	27.2	295	.188

Note: Gage Factor 0.84

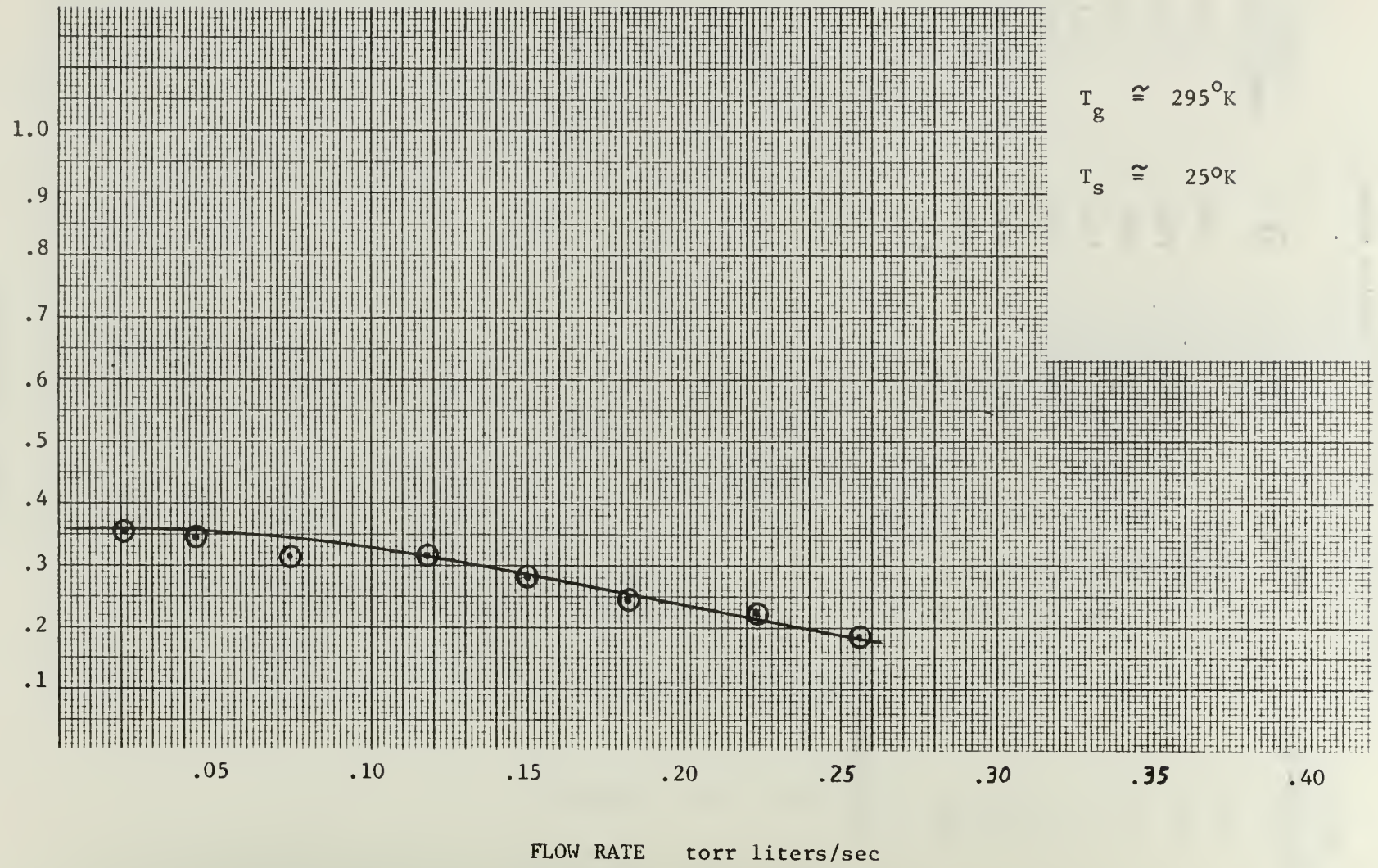

FIGURE 6. CAPTURE COEFFICIENT vs FLOW RATE FOR ARGON

5.2 Comparison with Published Data.

Tables IV, V, and VI show typical reported capture coefficients for carbon dioxide, nitrogen, and argon. The capture coefficients of carbon dioxide and nitrogen compare favorably with those published. In the case of argon the capture coefficients compare favorably with that of Everly's (5) at .1236 torr-liters/sec, but are very low compared to the other data listed in Table VI.

Investigators such as Yu and Soo (6) have stated that for CO_2 the capture coefficient is independent of cryosurface temperature below 80°K. In this respect this work does not agree with published data.

Table IV

Typical Reported Capture Coefficients of Carbon Dioxide

Flow $\frac{\text{torr liters}}{\text{sec}}$	T_s °K	T_g °K	Capture Coefficient	Reference
0.00356	19	297	0.65	5
0.060	27.9	296	0.559	this work
0.158	28.8	296	0.464	this work
0.208	28.3	296	0.408	this work
0.219	24	294	0.39	5
0.244	37.5	291	0.368	this work
not reported	10	300	0.77	7
not reported	10	300	0.75	2
not reported	20	300	0.62	7
not reported	20	300	0.63	2
not reported	20	300	0.64	8
variable	86	300	0.58	9
not reported	77	300	0.63	2
not reported	77	300	0.62	10
0.027	89.4	295	0.589	this work
0.0798	77	300	0.60	11
0.103	93.6	294	0.467	this work
0.185	90.2	299	0.411	this work
0.226	82	297	0.51	5
0.399	77	300	0.42	11

Table V

Typical Reported Capture Coefficients of Nitrogen

Flow $\frac{\text{torr liters}}{\text{sec}}$	T_s °K	T_g °K	Capture Coefficients	Reference
0.00226	25	300	0.62	3
0.00383	20	298	0.63	5
0.05	25	300	0.64	3
0.05	27.7	293	0.552	this work
0.102	34.9	293	0.52	this work
0.104	25	300	0.54	3
0.158	25	300	0.47	3
0.164	34.6	292	0.447	this work
0.2042	24	299	0.52	5
0.216	25	300	0.44	3
0.218	33.7	292	0.369	this work
0.425	25	300	0.28	3
0.433	30	295	0.241	this work
not reported	10	300	0.66	7
not reported	20	300	0.61	7
not reported	20	300	0.60	2
variable	33	294	0.65	9

Table VI

Typical Reported Capture Coefficients of Argon

Flow $\frac{\text{torr liters}}{\text{sec}}$	T_s °K	T_g °K	Capture Coefficients	Reference
not reported	10	300	0.68	7
not reported	20	300	0.65	7
not reported	20	300	0.66	2
.00332	19	297	0.68	5
.021	26.6	294	0.355	this work
.1236	25	297	0.25	5
.150	25.6	295	0.28	this work

6. Uncertainty Analysis.

To analyze the uncertainties in the determination of the capture coefficient the method of Kline and McClintock (13) was used. In this method each variable is considered to have a normal distribution. From equation (4.3) the condensation coefficient is essentially a linear function of several independent variables

$$f_g = \frac{Q_L}{\Delta P (G.F.) A_s T_L} \left[\frac{2\pi M T_g}{R}\right]^{\frac{1}{2}} \qquad (4.3)$$

where $\left[\frac{2\pi M}{R}\right]^{\frac{1}{2}}$ is a constant and Q_L is equal to $\dot{P}_L V_L$. In addition the variable β for conductance effects must be considered. V_L, A_s, and β are all averages of several measurements and the uncertainties were judged from the differences in measurements.

T_L and T_g were measured using thermocouples calibrated with water-ice and liquid nitrogen junctions. Because T_L and T_g were at or near ambient temperature and were checked against a standard thermometer the value of $\pm$ 0.5°K is a conservative estimate. As can be seen from Table VII their values are negligible in comparison with the other variables.

ΔP was measured with an ionization gage which has a 2% accuracy as stated by the manufacturer.

J. H. Leck (14) reports that the gage factors reported by various investigators were within $\pm$ 20% and that there were variations between several identical gages tested under the same conditions. A value of 0.10 was therefore assigned for the uncertainty of G. F.

$\dot{P}_L$, the pressure rise used to measure the flow rate, was measured with a thermocouple gage. The average difference found was two parts in twenty yielding a fraction of 0.10. There are then eight independent variables that must be taken into consideration.

$$\frac{\Delta f}{f} = \left[\left(\frac{\Delta V_L}{V_L}\right)^2 + \left(\frac{\Delta A_s}{A_s}\right)^2 + \left(\frac{\Delta \beta}{\beta}\right)^2 + \left(\frac{\Delta T_L}{T_L}\right)^2 + \left(\frac{\Delta T_g}{T_g}\right)^2 + \left(\frac{\Delta(\Delta P)}{\Delta P}\right)^2 + \left(\frac{\Delta \dot{P}_L}{\dot{P}_L}\right)^2 + \left(\frac{\Delta G.F.}{G.F.}\right)^2\right]^{\frac{1}{2}} \quad (6.1)$$

The values of the variables and their uncertainties are listed in Table VII.

Table VII

Uncertainties in Measured Values

Quantity	Value	Uncertainty	$\frac{\Delta X}{X}$
V_L	4350 cm^3	50 cm^3	0.011
A_s	3300 cm^2	50 cm^2	0.015
β	7780 cm^2	500 cm^2	0.064
T_L	300°K	0.5°K	0.002
T_g	300°K	0.5°K	0.002
ΔP	Variable	----	0.02
G.F.	1.00	.10	0.10
$\dot{P}_L$	Variable	----	0.10

Substituting the values of $\frac{\Delta X}{X}$ from Table VII into equation (6.1) yields:

$$\frac{\Delta f}{f} = 0.152 \quad (6.2)$$

7. Conclusions.

The capture coefficients of carbon dioxide, nitrogen, and argon depend upon the flow rate when the gas throughput Q_L is greater than .05 torr-liters/sec. The three gases tested have different characteristics and therefore this conclusion may be extrapolated to include most gases. Below .05 torr-liters/sec the capture coefficient appears to be constant for a given gas. This may explain the reason for most investigators stating that the capture coefficient is a constant value for a given gas.

The capture coefficient of carbon dioxide is dependent upon the cryopanel temperature above a flow rate of .05 torr-liters/sec. The effect is not large and for most design purposes may be ignored compared to the accuracy of the capture coefficient at a given temperature. See equation (6.2). The effect can not be ignored when the cryopanel design is critical for a specific application.

As stated in Section (5.1.b) the capture coefficient of nitrogen may also depend upon the temperature of the cryopanel.

The results of this work indicate the need for further investigations into capture coefficients of gases. The best pressure and temperature measuring devices should be used to reduce the errors in the capture coefficient. It must be realized that the present day knowledge may not be adequate. For example, a form of mass spectrometer may be the best pressure measuring device, however, this apparatus requires a knowledge of the sensitivity to various gases. This is where the knowledge is lacking. (14,15)

It is also concluded that the study of capture coefficients should be divided into various flow regimes. Below 0.05 torr-liters per second the capture coefficients appear to be constant for a given gas, this could be designated Regime I. Regime II would begin at 0.05 torr-liters per second

where the capture coefficients begin to decrease with increasing flow rates. See Figure 7.

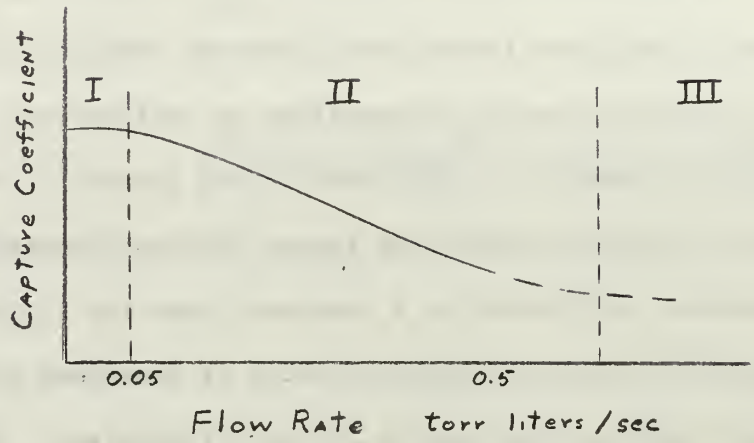

Fig. 7. Flow Regimes

Dawson (2) indicates that pumping speed will increase upon entry into the transition to the continuum region from free molecular flow region. The flow rates studied in this report do not indicate where this point would be, however, this could be designated Regime III. The designers of a cryopumping system could then utilize the proper capture coefficient for the regime in which they are working.

BIBLIOGRAPHY

1. Steinherz, H. A., High Vacuum Engineering, Reinhold Publishing Corp., 1963.

2. Dawson, J. P., and Haygood, J. D., "Cryopumping", Cryogenics, Vol. 5, April, 1965.

3. Bevan, J. A., "Capture Coefficients of Nitrogen on a Cryogenically Cooled Panel", M. S. Thesis Naval Postgraduate School, June, 1967.

4. Scott, R. B., Cryogenic Engineering, D. Van Nostrand Company, Inc., 1959.

5. Everly, V. R., "The Bare Surface Effect in Cryogenic Pumping", M. S. Thesis, Naval Postgraduate School, Sept., 1967.

6. Yu, J. S., and Soo, S. L., "Interaction of Gases with Condensed Phase", Journal of Vacuum Science and Technology, Vol. 3, No. 1, Jan/Feb, 1966.

7. Dawson J. P., "Capture Coefficients of Six Common Gases", Technical Report, AEDC-TDR-64-68, May, 1964.

8. Dawson, J. P., Haygood, J. D., and Collins, J. A., Jr., "Temperature Effects on the Capture Coefficients of CO_2, N_2, and A", Advances in Cryogenic Engineering, Vol. 9, Plenum Press, Inc., 1963.

9. Tedeschi, L. C., "Capture Coefficients of Carbon Dioxide and Nitrogen Gas on A Cryogenic Cooled Surface", M. S. Thesis, Naval Postgraduate School, May, 1966.

10. Brown, R. F., and Wang, E. S. J., "Capture Coefficients of Gases at 77°K", Advances in Cryogenic Engineering, Vol. 10, Plenum Press, Inc., 1965.

11. Wang, E. S. J., Collins, J. A., Jr. and Haygood, J. D., "General Cryopumping Study", Advances in Cryogenic Engineering, Vol. 7, Plenum Press, Inc., 1962.

12. Albero, C. M., "Design and Development of a Cryogenic Pumping Evaluation Facility", M. S. Thesis, Naval Postgraduate School, 1965.

13. Kline, S. J., and McClintock, F. A., "Uncertainties in Single Sample Experiments", Mechanical Engineering, January, 1953.

14. Leak, J. H., Pressure Measurements in Vacuum Systems, Unwin Brothers Limited, 1957.

15. Dushman, S., Lafferty, J. M., Scientific Foundations of Vacuum Technique, John Wiley & Sons, Inc., 1962.

16. LaChance, G. M., "The Theory and Construction of a Liquid Helium Cryopump", M. S. Thesis, Naval Postgraduate School, 1964.

17. Powell, R. L., and Sparks, L. L., "Available Low Temperature Thermocouple Information and Services", NBS Report 8750, February, 1965.

18. Dayton, B. B., "Outgassing Rate of Contaminated Metal Surfaces", 1961 Vacuum Symposium Transactions, Pergamon Press, Inc., 1962.

Appendix A

General Description of Systems

The system described below was built and modified at the Naval Postgraduate School during the past four years by LaChance (16), Albero (12), Tedeschi (9), and Bevan (3). The basic system is shown in Figures 8, 9, and 10. Photographs of the system may be found in references (3), (5), and (9).

a. Main Vacuum Chamber.

The vacuum chamber is a modified 40" diameter stainless steel horizontal furnace tank, Model 2555, manufactured by the National Research Corporation. The description of the modifications is included in reference 16. The chamber volume is 994 liters.

Contained within the chamber is the radiation shielding and the cryopanel. The shielding consists of one 33" diameter, 36" long, type 304 stainless steel cylindrical shell with two 36" diameter end shields. All shields are singly embossed on the outer surface with appropriate fill and vent line connections. The shields were manufactured by Dean Products, Inc., Brooklyn, New York. The volumetric capacity of the shields is 33 liters.

The cryopanel was manufactured by Dean Products, Inc. It consists of two 12" by 20" type 304 stainless steel sheets welded at the edges. One side of the panel is embossed and the panel has been electropolished.

b. Vacuum Pumping System.

A NRC, Model HS6-1500, four-stage, fractionating diffusion pump was used to pump down the chamber. The pumping fluid used was Dow Corning 704. The pump is rated at 1500 liters/sec. with a blank off pressure of about 10^{-7} torr. A liquid nitrogen, NRC Series 0315, cold trap

was utilized with the diffusion pump.

The diffusion pump was backed by an NRC Model 100S, single stage mechanical pump with a blank off pressure of 10 to 15 microns and a pumping capacity of 100 CFM.

c. Instrumentation.

1. Pressure measurements were made with Vacuum Electronics Corporation thermocouple gages down to 10^{-3} torr. Below 10^{-3} torr the pressure was measured by a Bayard-Alpert ionization gage located on the chamber wall. A General Electric cold cathode trigger gage was available to use as a comparison for the ionization gage.

2. Temperature measurements were made with Teflon-insulated 24 gage, copper-constantan thermocouples installed on the cryopanels and radiation shields as shown in Figure 10. A National Bureau of Standards computer program (17) was used to generate a thermocouple temperature table for the installed thermocouples. The thermocouples were read using a differential amplifier fed into a digital voltmeter with automatic print out.

3. All necessary electrical controls are located in a desk top panel. In event of high chamber pressure, high diffusion pump temperature, or power failure the system automatically shuts down and isolates the chamber.

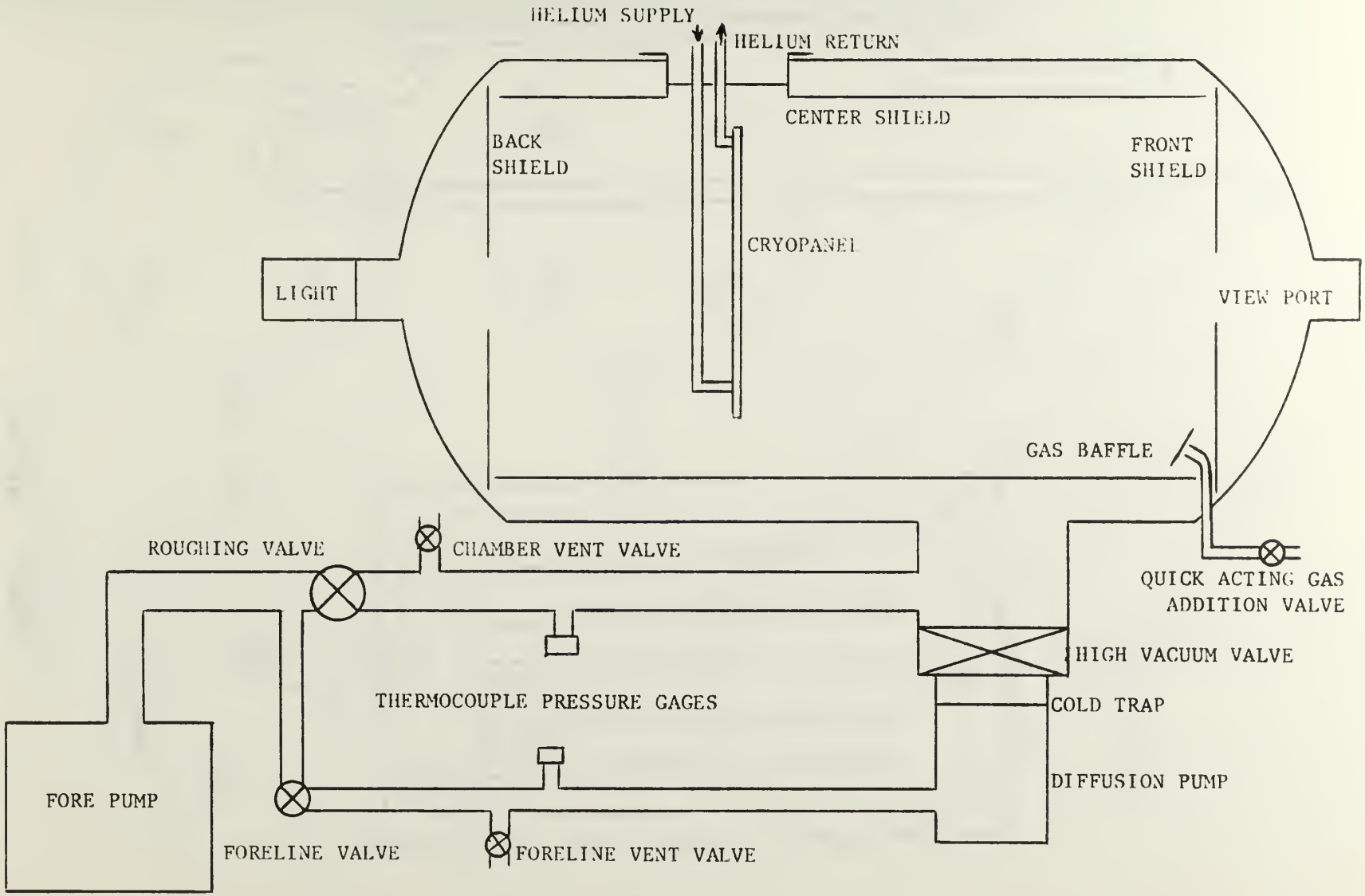

FIGURE 8. SCHEMATIC OF THE SYSTEM

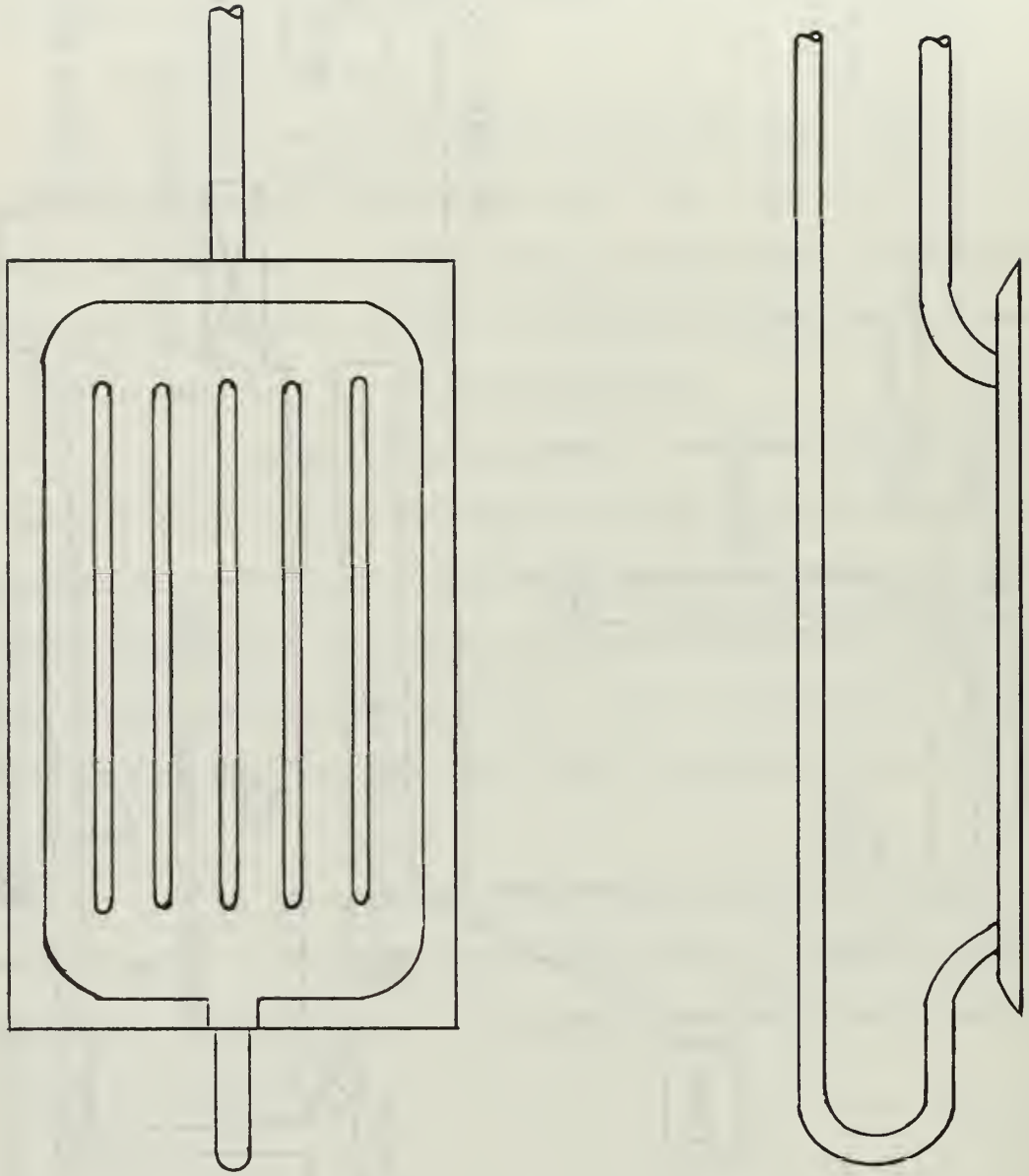

FIGURE 9. CRYOPANEL

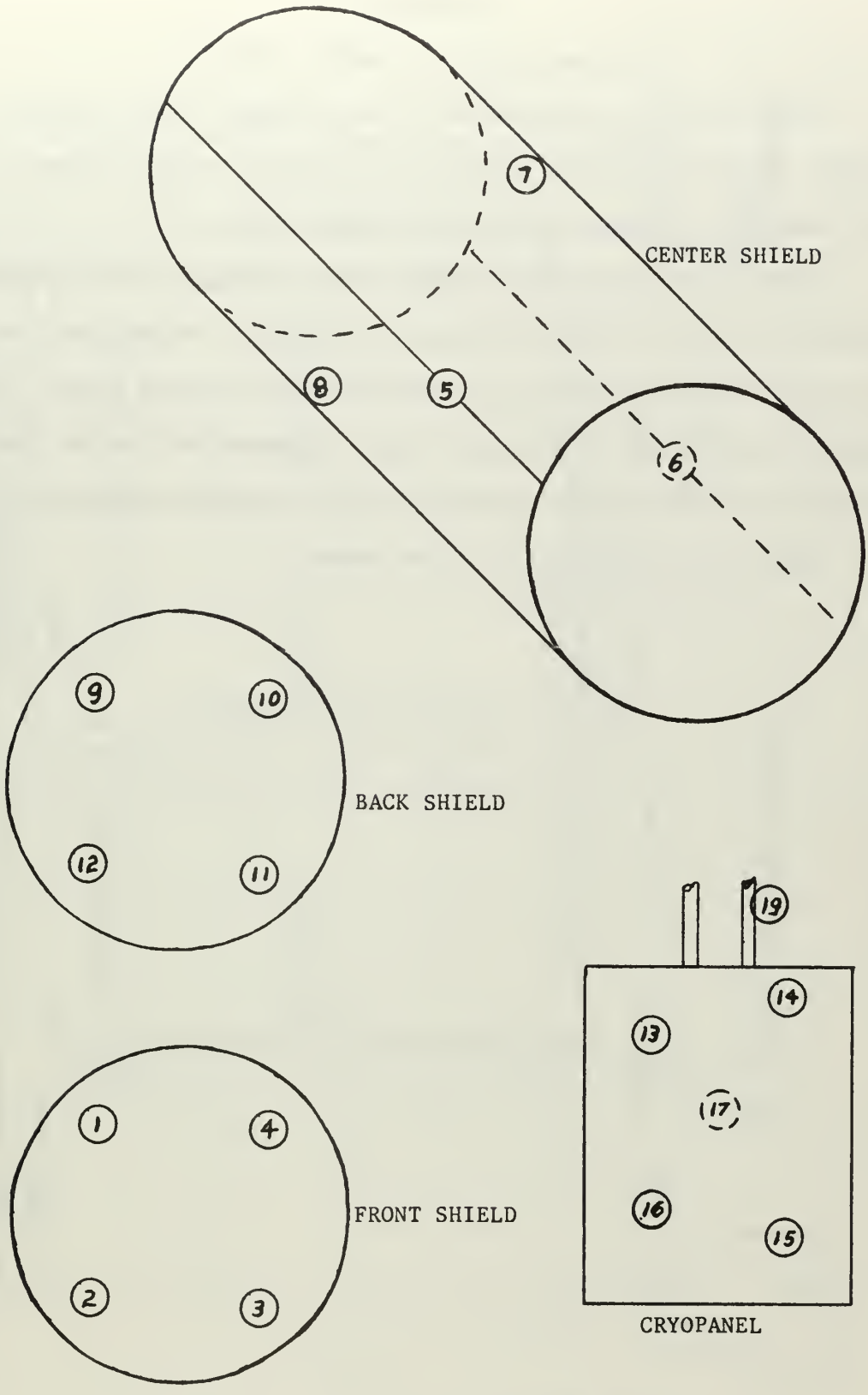

FIGURE 10. LOCATION OF THERMOCOUPLES

Appendix B

Cryogenic Fluid Transfer System

Liquid Helium is transferred to the cryopanel from a Arthur D. Little, ADL-Collins Helium Liquifier via vacuum jacketed transfer lines. The lines were designed and built by Tedeschi (9).

Lines are available to transfer liquid nitrogen to the radiation shields as well as the diffusion pump cold trap. Motive power for the liquid nitrogen is provided by pressurizing a 172 liter dewar. Initial pressure is obtained by applying 8 psig of gaseous helium and then the normal boil off of liquid nitrogen maintains adequate pressure.

Figure 11 is a schematic of the system.

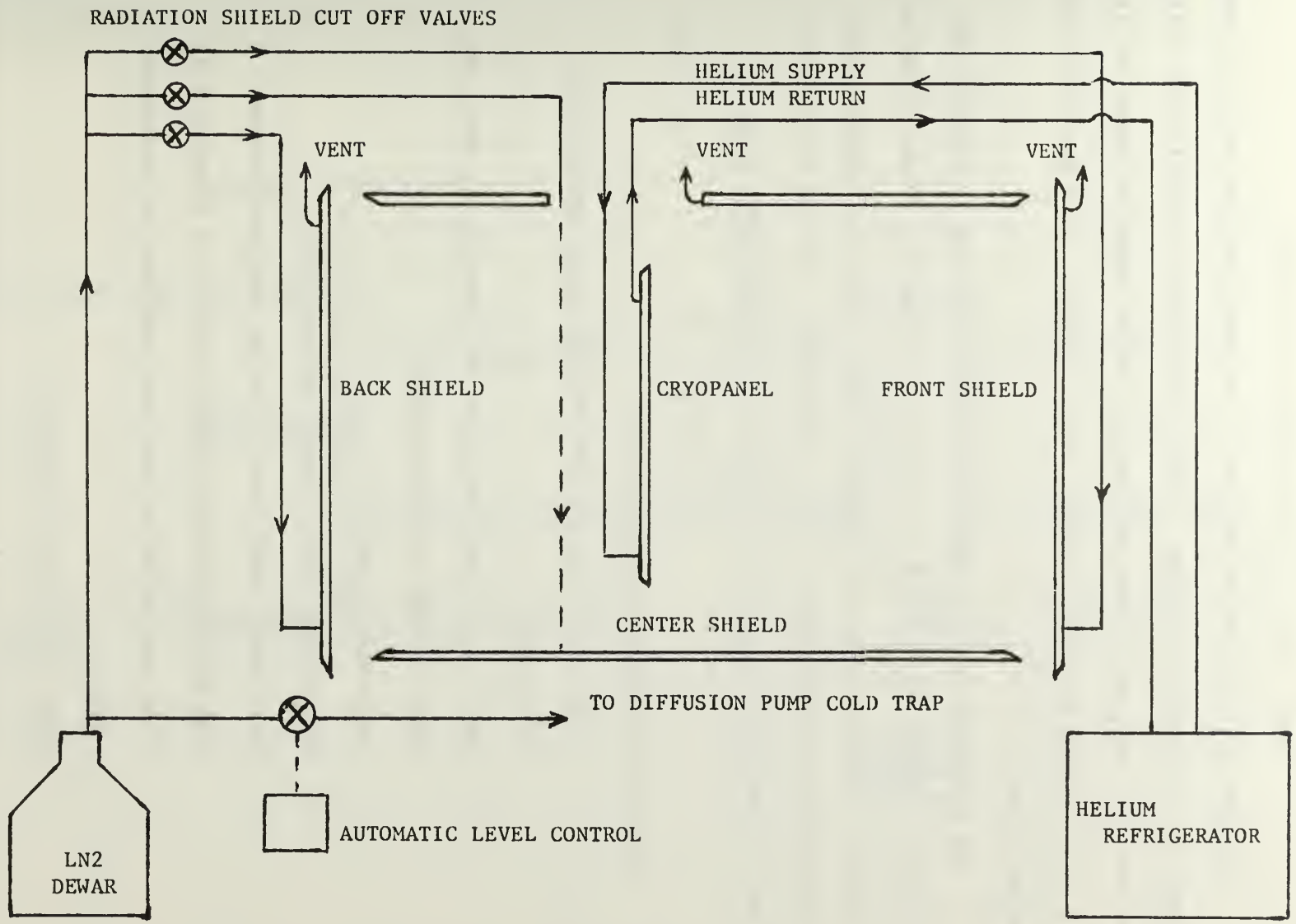

FIGURE 11. SCHEMATIC OF CRYOGENIC FLUID TRANSFER SYSTEM

Appendix C

Gas Addition and Flow Measurement System

The gas addition system consists of an auxiliary tank with a diffusion pump and a mechanical forepump. Appropriate valves and piping are installed between the auxiliary volume and the high vacuum system as shown in Figure 12. This system is used to measure the flow rate of test gas to the high vacuum system.

The procedure used to determine the flow rate was to evacuate the auxiliary volume, which was 4.35 liters, including the volume of the appropriate lines, valves, and ionization gage. Then the variable leak valve was set at the desired rate. The pressure rise was then recorded from a thermocouple gage and the flow rate was calculated from

$$Q_L = \dot{P} V \qquad (C.1)$$

Specific operating procedures were:

1. Insure gas isolation and test gas quick acting valve are closed.
2. Open the variable leak valve and valve 1, 2, and 3 and pump down the auxiliary system.
3. Shut valves 2 and 3.
4. Set variable leak valve to desired valve.
5. When system stabilizes, close the auxiliary system high vacuum valve and record the rate of pressure rise.
6. Close gas isolation valve and pump down the auxiliary system.
7. Close valve 1 and open valve 3.
8. The known gas flow rate is then re-established to the main vacuum system by opening the gas isolation valve and the test gas quick acting valve.

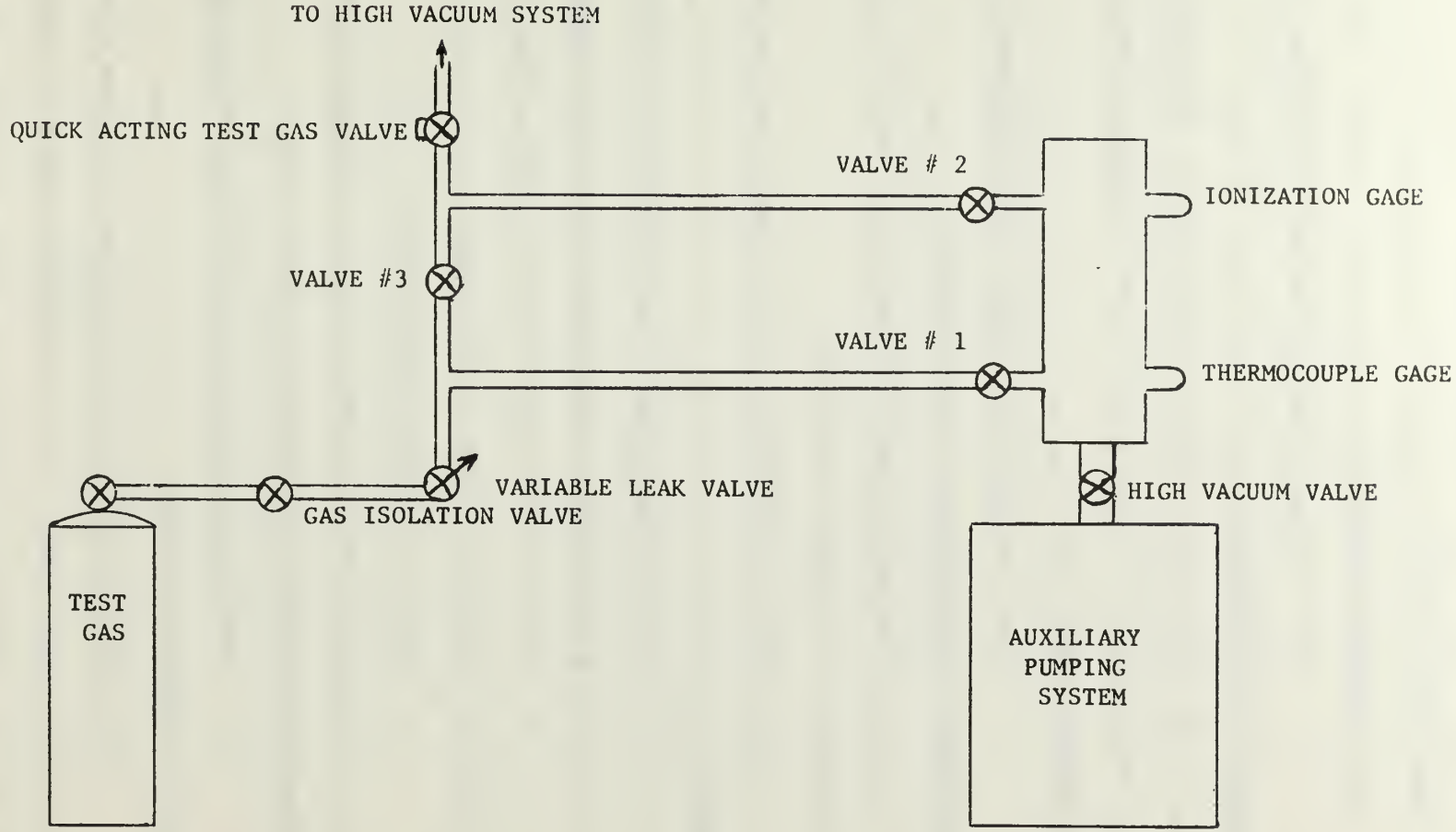

FIGURE 12. GAS ADDITION AND FLOW MEASUREMENT SYSTEM

Appendix D

Operating Procedures

I. Main Vacuum System.

A. Initial pump down

1. Check the oil level of the two bearing caps and the pumping chamber of the forepump.

2. Turn on the forepump cooling water. The water is thermostatically controlled at the pump and will not flow unless the pump temperature reaches 180°F.

3. Close the electrical breakers and disconnect switches for the forepump, diffusion pump, and solenoids.

4. Open the air supply valves to the solenoids. Insure that air pressure of 90 psig is available.

5. Check to see that all doors, ports, and vent valves are closed.

6. At the control panel place overpressure switches on "out".

7. At the control panel energize the power to solenoids.

8. At the control panel close the quick acting test gas valve and open the foreline and high vacuum valve.

9. Open the roughing valve manually.

10. At the control panel start the forepump and monitor the chamber pressure with the chamber thermocouple gage.

11. Turn on cooling water to the diffusion pump and cold cap. Close the quick cool valve.

12. When the tank pressure reaches 70 microns start the diffusion pump at the control panel. The pump requires about 20 minutes to become operational. Monitor the foreline pressure with the foreline thermocouple pressure gage. When there is a temporary pressure rise in foreline pressure

and a rapid decrease in chamber pressure the diffusion pump is operating.

13. When the diffusion pump is in operation, close the roughing valve to prevent backstreaming of forepump oil.

14. When the tank pressure goes below 1 micron, energize the ionization gage to monitor the chamber pressure.

15. When the tank pressure goes below 10^{-4} torr energize the liquid nitrogen level control valve to the cold trap to reduce backstreaming of diffusion pump oil.

16. Regulate the diffusion pump cooling water so that the return line is about 110°F (warm to the hand).

17. When leaving the system unattended, place the ionization gage selector on 10^{-4} torr and place the overpressure protection switch on "in".

If the system has been out of operation for a long period of time it may take three or four days to pump down to base operating pressure. Normally the system will pump down in approximately 10 hours. The foreline pressure should be on the order of 10 microns and the tank pressure should be on the order of 2×10^{-7} torr.

B. To open the chamber

1. Shut the high vacuum valve.

2. Open the chamber vent valve. If the chamber is to open only for a short time use dry nitrogen gas to bring chamber to atmospheric pressure. This will assist in the subsequent pumpdown.

3. When pressure is equalized open the chamber.

4. Keep the forepump and diffusion pump operating.

C. To re-evacuate chamber

1. Shut the chamber vent valve.

2. Shut the foreline valve.

3. Open the roughing valve.

4. When the chamber pressure goes below 70 microns close the roughing valve and open the foreline valve and the high vacuum valve.

D. To secure the system.

1. Shut the high vacuum valve.

2. De-energize the diffusion pump and turn on the quick cool water.

3. When the diffusion pump is cool, shut the foreline valve and secure the forepump.

4. Open the chamber vent valve and the foreline vent valve and equalize the pressure; then close the valves.

5. Secure all cooling water.

6. Secure air to solenoids.

7. Secure all electrical power.

II. Cryogenic Transfer System.

A. Liquid Nitrogen

1. Connect liquid nitrogen dewar to cryogenic line with rubber tubing.

2. Pressurize dewar with helium or gaseous nitrogen to 8 psig.

3. Energize diffusion pump cold trap automatic level control valve.

4. To fill radiation shields

a. Insure Armaflex connections fit tightly around supply lines.

b. Open the Jamesbury transfer valves and observe exhaust from shield vents.

c. Monitor shield thermocouples to determine the liquid level.

d. Reduce the liquid flow when shields are half full to prevent geysering from the vent lines.

e. It will be necessary to maintain a flow to the shields to replace evaporation losses.

B. Helium transfer.

1. Pump vacuum jackets of the transfer lines to approximately 15 microns.

2. To cool the cryopanel follow the instructions in the Operation and Maintenance Manual provided by the manufacturer.

3. To shut down system

a. Push both compressor switches off.

b. Push helium supply switch off.

c. Pull helium recovery switch on.

d. Push pre-cool switch off.

e. Turn off LN_2 dewar.

f. When LN_2 line de-ices, remove line from system and connect refrigerator line.

Appendix E

Model Analysis of ΔP

In order to insure that the measured pressure drop is in fact the pressure drop derived in equation (4.1), a model was proposed and analyzed by Tedeschi in 1966, and improved by Bevan in 1967 (9, 3). The complete analysis is included here since it is deemed so important to the experimental method of determining capture coefficients.

The system consists of a chamber in which is mounted a cylindrical radiation shield, two circular disk end shields and a gas addition system. The actual system is described in Appendix A. The model as shown in Figure 13 consists of three volumes. The chamber is divided into an inner volume V_i and an outer volume V_o by the radiation shielding. Conductance between the two volumes consists of two circular viewing ports in the end shields and a clearance between the end shields and the cylindrical shield. The gas addition volume V_a consists of tubing leading the gas from the controlled leak supply to the inner volume. Referring to Figure 13, the volumes, temperatures, and molecular flow rates that must be considered are:

V_a - Volume of piping between gas injection stop valve and chamber

V_i - Volume of the chamber inside the radiation shielding

V_o - Volume between the shielding and the tank wall

T_o - Mean temperature of tank wall and the radiation shielding

T_a - Temperature of the wall of the piping containing V_a

T_i - Temperature of the gas in V_i

T_L - Temperature of the gas admitted to V_a

$\dot{N}_L$ - Molecules/sec of controlled gas entering lines to the chamber

$\dot{N}_{ai}$ - Molecules/sec of controlled gas entering the inner volume V_i from V_a

$\dot{N}_c$ - Molecules/sec of condensable gas captured by the cryosurface

$\dot{N}_{io}$ - Molecules/sec of gas entering the outer volume V_o from V_i

$\dot{N}_D$ - Molecules/sec of condensable gas pumped by the diffusion pump and cryogenic trap

$\dot{N}_{ra}$, $\dot{N}_{ri}$, $\dot{N}_{ro}$ - Molecules/sec of residual condensable gas from leakage into the chamber and outgassing of materials within the chamber

$\dot{N}_i$ - Summation of all gas fluxes into V_i

$\dot{N}_o$ - Summation of all gas fluxes into V_o

$\dot{N}_a$ - Summation of all gas fluxes into V_a

Expressions for each of the molecular flow rates are developed in terms of measurable quantities as follows:

(1) $\dot{N}_i$, $\dot{N}_o$, $\dot{N}_a$

From the ideal gas law

$$N = \frac{PVN_A}{RT}$$

$$\dot{N} = \frac{1}{k}\frac{d}{dt}\left[\frac{PV}{T}\right]$$

The gases all occupy the same constant volumes. As will be seen later, the temperature in any given volume must be assumed constant. Therefore,

$$\dot{N} = \frac{V}{kT}\dot{P}$$

and

$$\dot{N}_i = \frac{V_i}{kT_i}\dot{P}_i \qquad \text{(E.1)}$$

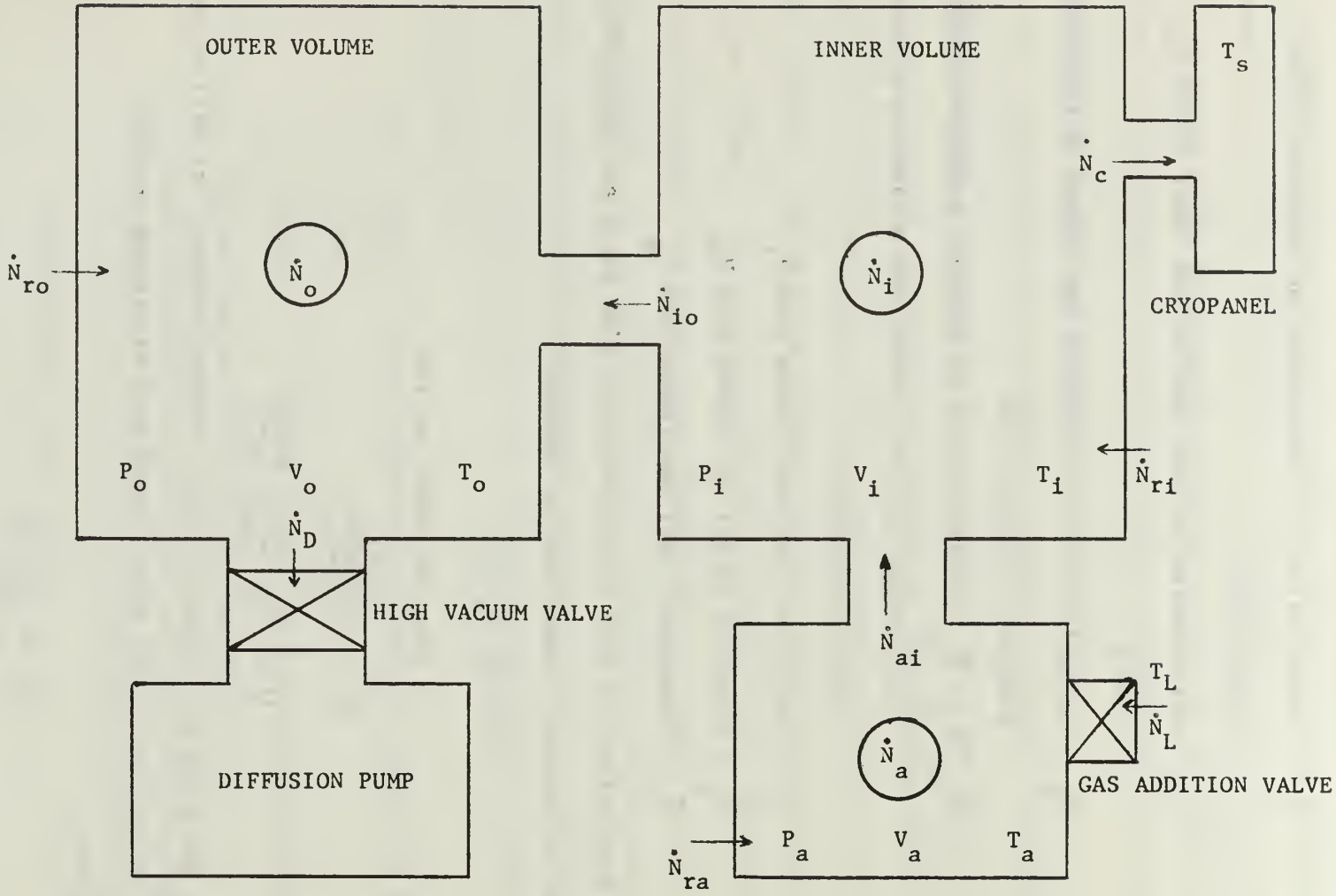

FIGURE 13. MODEL FOR ANALYSIS OF PRESSURE DROP

$$\dot{N}_o = \frac{V_o}{KT_o} P_o \qquad (E.2)$$

$$\dot{N}_a = \frac{V_a}{KT_a} P_a \qquad (E.3)$$

(2) $\dot{N}_L$

The flow of controlled gas is

$$\dot{N}_L = \frac{1}{K} \frac{d}{dt}\left[\frac{P_L V_L}{T_L}\right]$$

where P_L and T_L are the pressure and temperature at the inlet to the gas addition piping and are constant, so that:

$$\dot{N}_L = \frac{P_L \dot{V}_L}{K T_L} = \frac{Q_L}{KT_L} \qquad (E.4)$$

(3) $\dot{N}_{ai}$, $\dot{N}_{io}$

From kinetic theory, the number of molecules incident on a surface per unit time is

$$\dot{N} = \frac{PA}{[2\pi m K T]^{\frac{1}{2}}} \qquad (3.4)$$

Then

$$\dot{N}_{ai} = C_a \left[\frac{P_a}{\sqrt{T_a}} - \frac{P_i}{\sqrt{T_i}}\right] \qquad (E.5)$$

where

$$C_a = \frac{A_{ai}}{[2\pi m K]^{\frac{1}{2}}}$$

and A_{ai} is the area through which the gas flows as it travels from V_a to V_i. Similarly,

$$\dot{N}_{io} = C_i \left[\frac{P_i}{\sqrt{T_i}} - \frac{P_o}{\sqrt{T_o}}\right] \qquad (E.6)$$

(4) $\dot{N}_c$

The expression for the flow to the cryopanel is given by equation (3.16)

$$\dot{N}_c = \frac{A_s}{[2\pi k m]^{\frac{1}{2}}} \left[\frac{f_g P_i}{\sqrt{T_i}} - \frac{f_s P_s}{\sqrt{T_s}} \right] \tag{3.16}$$

(5) $\dot{N}_D$

The volumetric pumping speed of a diffusion pump can be considered constant over the pressure range of interest here. The pumping speed curve for the pump employed in this system is shown in Figure 14. Since pressure change has no effect on the pumping speed,

$$\dot{N}_D = \frac{P}{KT} \dot{V}_D \tag{E.7}$$

If, as in this system, the diffusion pump is used with a cryogenic trap, the limited conductance of the trap will reduce V_D and

$$\dot{N}_D = \left[\frac{\alpha \dot{V}_o}{K T_o} \right] P_o \tag{E.8}$$

where α is an efficiency factor.

(6) $\dot{N}_r$

After exposure to atmospheric air for several hours, the amount of gas readily available for desorption from a surface at room temperature amounts to many molecular layers. Although the outgassing rate of a material is time dependent, after exposure to vacuum for considerable periods, the variation with time is small. For example, Dayton (18) shows that after ten hours of vacuum pumping, the outgassing rate for a stainless steel surface is 1×10^{-8} torr liter/sec-cm^2 and is decreasing very slowly. Since the time required for measurements is small, the outgassing rate will be considered constant.

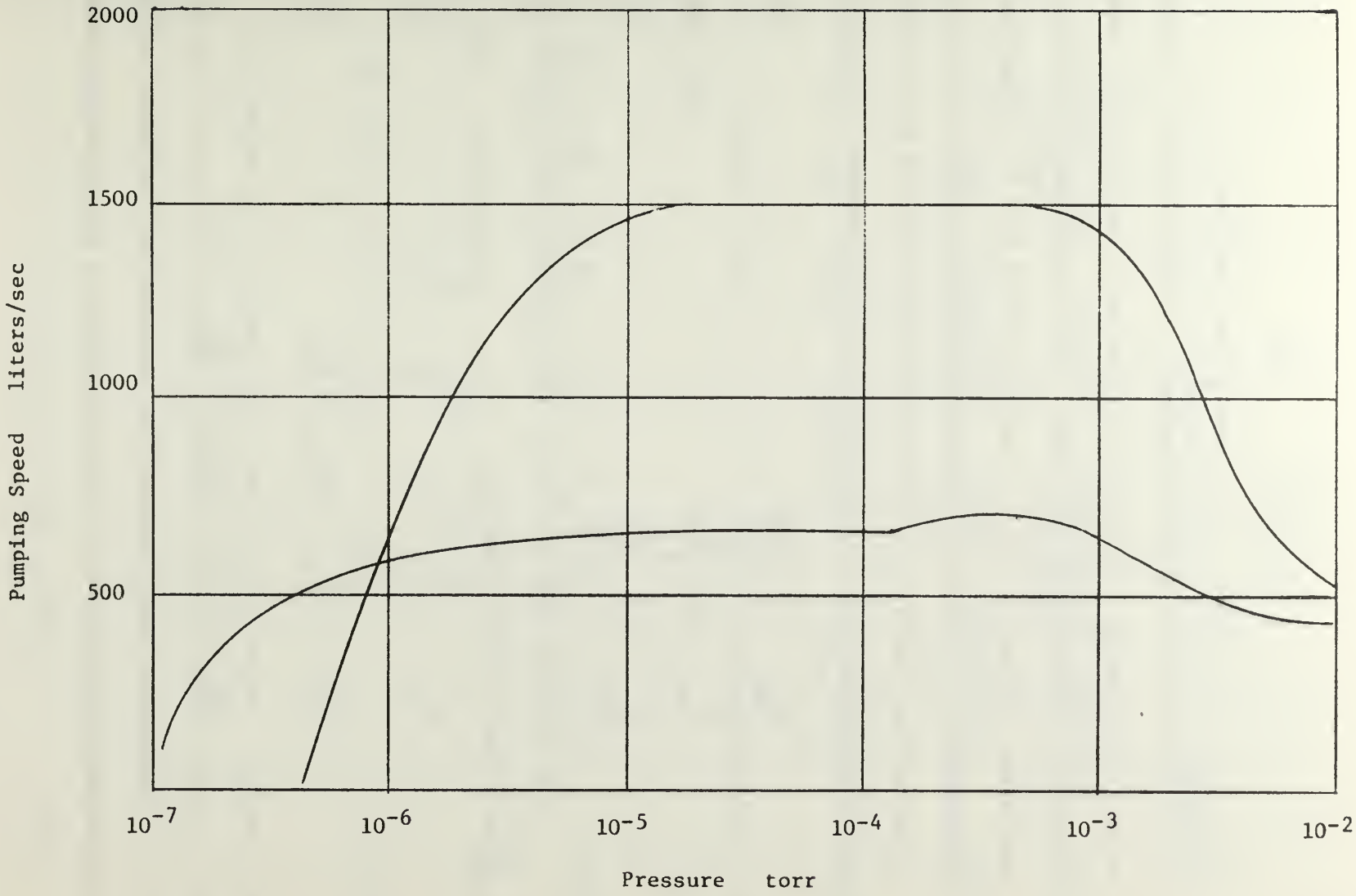

FIGURE 14. DIFFUSION PUMP CHARACTERISTICS

$$\dot{N}_r = \frac{1}{K} \frac{d}{dt} \left[\frac{PV}{T} \right] = \frac{Q_r}{K T_r} \tag{E.9}$$

where Q_r is the outgassing rate from a given surface.

The diffusion of a gas through metal is proportional to the square root of the pressure. The rate of diffusion is small and the pressure changes in the system are very small. The leakage rate is therefore considered constant and will be included in the term for outgassing. Measurements of the combined effects of outgassing and leakage in this system at room temperature indicated that these effects were constant over the short periods of time required for measurements. Therefore,

$$\dot{N}_{ra} = \frac{Q_{ra}}{K T_a} \tag{E.10}$$

$$\dot{N}_{ri} = \frac{Q_{ri}}{K T_i} \tag{E.11}$$

$$\dot{N}_{ro} = \frac{Q_{ro}}{K T_o} \tag{E.12}$$

The following equations result from molecular rate balances on the three volumes shown in Figure 13.

$$\dot{N}_i = \dot{N}_{ri} + \dot{N}_{ai} - \dot{N}_c - \dot{N}_{io} \tag{E.13}$$

$$\dot{N}_o = \dot{N}_{io} + \dot{N}_{ro} - \dot{N}_o \tag{E.14}$$

$$\dot{N}_a = \dot{N}_i + \dot{N}_{ra} - \dot{N}_{ai} \tag{E.15}$$

Substitution of the expressions developed for the terms in these equations and solution for the rate of pressure change in each volume yields

$$\dot{P}_i = \frac{Q_{ri}}{V_i} + \left[\frac{f_s A_s T_i}{V_i}\left(\frac{K}{2\pi m T_s}\right)^{\frac{1}{2}}\right] P_s + \left[\frac{C_i K T_i}{V_i \sqrt{T_o}}\right] P_o$$

$$+ \left[\frac{C_a K T_i}{V_i \sqrt{T_a}}\right] P_a - \left[\frac{C_a K T_i^{\frac{1}{2}}}{V_i} + \frac{f_g A_s}{V_i}\left(\frac{K T_i}{2\pi m}\right)^{\frac{1}{2}} + \frac{C_i K T_i^{\frac{1}{2}}}{V_i}\right] P_i \qquad \text{(E.16)}$$

$$\dot{P}_o = \frac{Q_{ro}}{V_o} + \left[\frac{C_i K T_o}{V_o T_i^{\frac{1}{2}}}\right] P_i - \left[\frac{\alpha \dot{V}_o}{V_o} + \frac{C_i K T_o^{\frac{1}{2}}}{V_o}\right] P_o \qquad \text{(E.17)}$$

$$\dot{P}_a = \frac{Q_{ra}}{V_a} + \frac{Q_L T_a}{V_a T_L} + \left[\frac{C_a K T_a}{V_a T_i^{\frac{1}{2}}}\right] P_i - \left[\frac{C_a K T_a^{\frac{1}{2}}}{V_a}\right] P_a \qquad \text{(E.18)}$$

By defining constants as in Table XIII, the equations above can be expressed as,

$$\dot{P}_i = A + a_1 P_o + a_2 P_a - [a_3 + a_4 + a_5] P_i \qquad \text{(E.19)}$$

$$\dot{P}_o = B + a_6 P_i - [a_7 + a_5] P_o \qquad \text{(E.20)}$$

$$\dot{P}_a = C + D + a_9 P_i - a_{10} P_a \qquad \text{(E.21)}$$

These are the equations which describe the system. They have been solved on an analog computer by Tedeschi (9), and curves similar to that shown in Figure 3, Section 4.1 have been obtained. Reference to Figure 3 and to equations (E.19), (E.20) and(E.21) yield the following solutions for steady state operations between times t_1 and t_2.

COEFFICIENT	EXPRESSION	COEFFICIENT	EXPRESSION
A	$\frac{Q_{ri}}{V_i} + \frac{f_s A_s T_i}{V_i}\left[\frac{K}{2\pi m T_s}\right]^{\frac{1}{2}} P_s$	a_4	$\frac{f_g A_s}{V_i}\left[\frac{K T_i}{2\pi m}\right]^{\frac{1}{2}}$
B	$\frac{Q_{ro}}{V_o}$	a_5	$\frac{C_i K T_i^{\frac{1}{2}}}{V_i}$
C	$\frac{Q_{ra}}{V_a}$	a_6	$\frac{C_i K T_o}{V_o T_i^{\frac{1}{2}}}$
D	$\frac{Q_L T_a}{V_a T_L}$	a_7	$\frac{\alpha \dot{V}_o}{V_o}$
a_1	$\frac{C_i K T_i}{V_i T_o^{\frac{1}{2}}}$	a_8	$\frac{C_i K T_o^{\frac{1}{2}}}{V_o}$
a_2	$\frac{C_a K T_i}{V_i T_a^{\frac{1}{2}}}$	a_9	$\frac{C_a K T_a}{V_a T_i^{\frac{1}{2}}}$
a_3	$\frac{C_a K T_i^{\frac{1}{2}}}{V_i}$	a_{10}	$\frac{C_a K T_a^{\frac{1}{2}}}{V_a}$

TABLE VIII COEFFICIENTS OF SYSTEM EQUATIONS

$$P_i(I) = \frac{a_{10}(a_7 + a_8)A + a_1 a_{10} B + a_2 (a_7 + a_8)(C + D)}{a_{10}(a_7 + a_8)(a_3 + a_4 + a_5) - a_1 a_6 a_{10} - a_2 a_9 (a_7 + a_8)} \quad \text{(E.22)}$$

$$P_o(I) = \frac{B}{a_7 + a_8} + \frac{a_6}{a_7 + a_8} P_i(I) \quad \text{(E.23)}$$

$$P_a(I) = \frac{C + D}{a_{10}} + \frac{a_9}{a_{10}} P_i(I) \quad \text{(E.24)}$$

At time t_2, the diffusion pump is isolated from the system and therefore, $a_7 = \dot{V}_D/V_o = 0$, and the equilibrium solutions are:

$$P_i(II) = \frac{a_{10} a_8 A + a_1 a_{10} B + a_2 a_8 (C + D)}{a_{10} a_8 (a_3 + a_4 + a_5) - a_1 a_6 a_{10} - a_2 a_3 a_9} \quad \text{(E.25)}$$

$$P_o(II) = \frac{B}{a_8} + \frac{a_6}{a_8} P_i(II) \quad \text{(E.26)}$$

$$P_a(II) = \frac{C + D}{a_{10}} + \frac{a_9}{a_{10}} P_i(II) \quad \text{(E.27)}$$

At time t_3, the gas inflow is abruptly halted and therefore, $D = Q_L T_a / V_L T_L = 0$. The equilibrium solutions are:

$$P_i(III) = \frac{a_{10} a_8 A + a_1 a_{10} B + a_2 a_8 C}{a_{10} a_8 (a_3 + a_4 + a_5) - a_1 a_6 a_{10} - a_2 a_8 a_9} \quad \text{(E.28)}$$

$$P_o(III) = \frac{B}{a_8} + \frac{a_6}{a_8} P_i(III) \quad \text{(E.29)}$$

$$P_a(III) = \frac{C}{a_{10}} + \frac{a_9}{a_{10}} P_i(III) \qquad (E.30)$$

The pressure drop in the inner volume is then

$$P_i(II) - P_i(III) = \frac{a_2 a_8 D}{a_8 a_{10}(a_3 + a_4 + a_5) - a_1 a_6 a_{10} - a_2 a_8 a_9} \qquad (E.31)$$

and substitution of the constants from Table XIII yields

$$P_i(II) - P_i(III) = \frac{Q_L T_i}{f_g A_s T_L} \left[\frac{2\pi M}{R T_i}\right]^{\frac{1}{2}} \frac{T_i}{T_L}$$

or

$$f_g = \frac{Q_L}{A_s [P_i(II) - P_i(III)]} \left[\frac{2\pi M}{R T_i}\right]^{\frac{1}{2}} \frac{T_i}{T_L} \qquad (E.32)$$

This is the same expression as equation (4.1) when it is considered that:

T_i is the temperature of the gas in the inner volume and is therefore equal to T_g.

P_i (II) is the equilibrium pressure with gas flow being admitted to the chamber and is therefore equal to P_e.

P_i (III) is the equilibirum pressure with no gas flow to the chamber and is therefore equal to P_g.

$$\Delta P = P_i \text{ (II)} - P_i \text{ (III)} = P_e - P_g$$

The experimentally observed pressure drop is therefore the same as that predicted by the theory providing the assumptions mentioned previously are valid and provided that the experimental pressure drop is measured in the inner volume V_i.

If the experimental pressure is measured in V_o, then the equations for the system predict

$$P_o(II) - P_o(III) = \frac{a_6}{a_8}\left[P_i(II) - P_i(III)\right] \tag{E.33}$$

Substitution of the constants results in

$$P_o(II) - P_o(III) = \left(\frac{T_o}{T_i}\right)^{\frac{1}{2}}\left[P_i(II) - P_i(III)\right] \tag{E.34}$$

which indicates that an application of the thermal transpiration effect is all that is required to relate the pressure drop measured in the outer volume to the pressure drop measured in the inner volume. The measurement of the pressure drop in the outer volume however, may not accurately reflect the rate of incidence of molecules on the cryosurface. If the conductance between the inner and outer volumes is not large, this conductance may have a significant effect on the measurement of the capture coefficient.

If the two volumes are considered connected by a conductance of area β, with the gas inflow into V_i as shown in Figure 15, the effect of the conductance may be determined in the following manner.

At steady state,

$$\frac{N_A P_L \dot{V}_L}{R T_L} = \frac{f A P_i}{\left[2\pi m k T_i\right]^{\frac{1}{2}}} \tag{E.35}$$

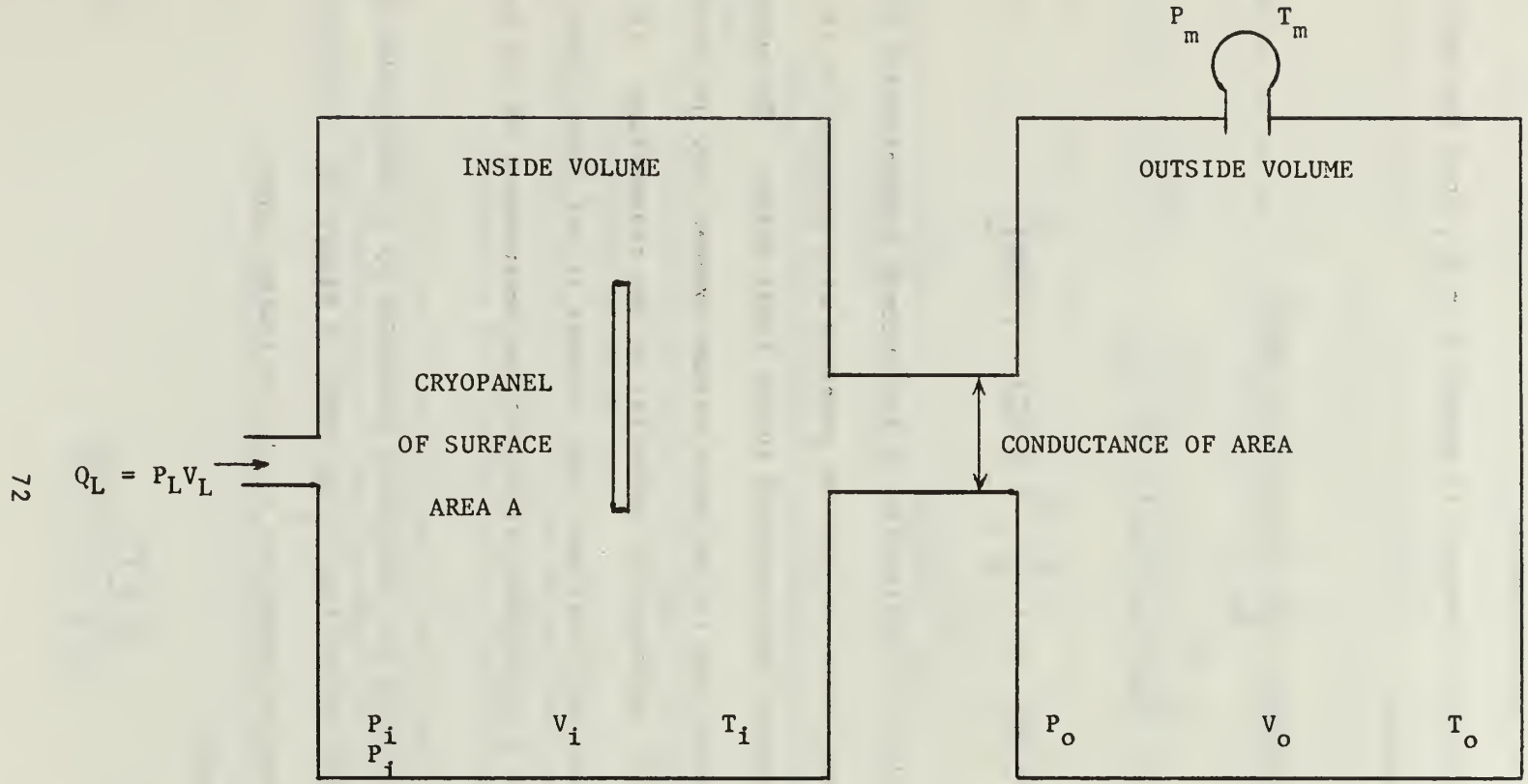

FIGURE 15. CONDUCTANCE EFFECTS

and

$$\frac{\beta P_o}{[2\pi m K T_o]^{\frac{1}{2}}} - \frac{\beta P_i}{[2\pi m K T_i]^{\frac{1}{2}}} = \frac{f A P_i}{[2\pi m K T_i]^{\frac{1}{2}}} \tag{E.36}$$

Solution of both equation for P_i and a subtraction yields,

$$P_o - \frac{N_A P_L \dot{V}_L}{\beta R T_L} (2\pi m K T_o)^{\frac{1}{2}} = \frac{N_A P_L \dot{V}_L}{A f R T_L} (2\pi m K T_o)^{\frac{1}{2}} \tag{E.37}$$

P_o can be eliminated by using thermal transpiration and if $T_m = T_L$, then,

$$P_m S_{th} - \frac{P_L \dot{V}_L}{\beta} = \frac{P_L \dot{V}_L}{A f} \tag{E.38}$$

where S_{th} = theoretical specific pumping speed liters/cm^2-sec; solving for the capture coefficient

$$f = \frac{\beta Q_L}{\beta A P_m S_{th} - A P_L \dot{V}_L} \tag{E.39}$$

If f* is the capture coefficient measured without any conductance effects, then equation (3.18) can be expressed as

$$f^* = \frac{Q_L}{A S_{th} P_m} \tag{E.40}$$

The ratio of these two capture coefficients is

$$\frac{f^*}{f} = \frac{\beta - f^* A}{\beta} \tag{E.41}$$

so that unless the product of the cryosurface area and the capture coefficient without conductance f* is small compared to the conductance area, the effect cannot be ignored. In order to eliminate the effect of limited conductance, it is desirable to measure the pressure in the volume containing the cryosurface.

Appendix F

Computer Program for Data Reduction

```
C      THIS PROGRAM CALCULATES THE CAPTURE COEFFICIENT CORRECTED
C      FOR CONDUCTANCE EFFECTS
C
       IMPLICIT REAL*8(A-H),REAL*8(O-Z)
      DIMENSION TIME(100),FG(100),FSTAR(100),TG(100),
     1TL(100),DELTAP(100)
II=44
DO 100 II=1,44
C
C      READ THE FOLLOWING INPUTS
C           NO=NUMBER OF DATA POINTS IN EXPERIMENT
C           Q=FLOW RATE IN TORR LITER/SEC
C           FORM=FORMULA WEIGHT
C           GF=GAGE FACTOR
C
   10 READ (5,11) NO,Q,FORM,GF
   11 FORMAT (1I10,3F10.0)
      IF (NO-2) 101, 100, 101
  101 CONTINUE
      DO 13 I=1,NO
C
C      READ THE FOLLOWING INPUTS
C           DELTAP=PRESSURE DROP IN TORR TIMES 10 +6 POWER
C           TIME=TIME IN SECONDS
C           TG=GAS TEMPERATURE IN DEGREES K
C           TL=LEAK TEMPERATURE IN DEGREES K
C
      READ (5,12)DELTAP(I),TIME(I),TG(I),TL(I)
   12 FORMAT(4F10.0)
   13 CONTINUE
      WRITE (6,14)
   14 FORMAT (1H1)
  600 WRITE (6,601)
  601 FORMAT(/,/,10X,9HFLOW RATE,/)
  602 WRITE(6,603) Q
  603 FORMAT(10X,F9.7)
  604 WRITE(6,605)
  605 FORMAT(/,/,12X,5HCAPCO,18X,4HTIME,/)
  606 DO 611 I=1,NO
  650 DELTAP(I)=DELTAP(I)*1.D-6
  651 TIME(I)=TIME(I)/60.
C
C      CALCULATE CAPTURE COEFFICIENT MEASURED WITH CONDUCTANCE
C
  607 FG(I)=(8.35D-5)*(Q/(DELTAP(I)*GF))*((DSQRT(TG(I)
```

```
     1*FORM))/TL(I))
C
CC      CALCULATE CAPTURE COEFFICIENT MEASURED WITHOUT CONDUCTANCE
C
  608 FSTAR(I)=1./((1./FG(I))+0.425)
  609 WRITE (6,610) FSTAR(I),TIME(I)
  610 FORMAT (10X,F10.8,10X,F10.5)
  611 CONTINUE
      GO TO 10
  100 CONTINUE
      END
```

INITIAL DISTRIBUTION LIST

		No. Copies
1.	Defense Documentation Center Cameron Station Alexandria, Virginia 22314	20
2.	Library Naval Postgraduate School Monterey, California 93940	2
3.	Naval Ship Systems Command Navy Department Washington, D. C. 20360	1
4.	Mechanical Engineering Department Naval Postgraduate School Monterey, California 93940	2
5.	Prof. Paul F. Pucci Mechanical Engineering Department Naval Postgraduate School Monterey, California 93940	5
6.	LT D. R. Breckenridge, USN USS CANBERRA (CAG2) % FPO San Francisco, Calif. 96601	2
7.	LCDR Vernon R. Everly, USN San Francisco Bay Naval Shipyard Mare Island, California 94592	1
8.	LCDR J. A. Bevan, USN Norfolk Naval Shipyard Portsmouth, Virginia 23709	1
9.	LT L. C. Tedeschi, USN Supervisor of Shipbuilding, U. S. Navy Bath Iron Works Bath, Maine 04530	1
10.	LCDR Carl Albero, USN Supervisor of Shipbuilding, U. S. Navy Bath Iron Works Bath, Maine, 04530	1
11.	LCDR G. M. LaChance, USN Naval Ship Systems Command (Code 1500) Navy Department Washington, D. C. 20360	1

Unclassified

Security Classification

DOCUMENT CONTROL DATA - R & D

(Security classification of title, body of abstract and indexing annotation must be entered when the overall report is classified)

1. ORIGINATING ACTIVITY *(Corporate author)*

Naval Postgraduate School, Monterey, California

2a. REPORT SECURITY CLASSIFICATION

Unclassified

2b. GROUP

3. REPORT TITLE

A Study of the Capture Coefficients of Nitrogen and Carbon Dioxide

4. DESCRIPTIVE NOTES *(Type of report and, inclusive dates)*

None

5. AUTHOR(S) *(First name, middle initial, last name)*

Breckenridge, Donald Roger

6. REPORT DATE	7a. TOTAL NO. OF PAGES	7b. NO. OF REFS
June 1968	74	18

8a. CONTRACT OR GRANT NO.	9a. ORIGINATOR'S REPORT NUMBER(S)
b. PROJECT NO. N/A	N/A
c.	9b. OTHER REPORT NO(S) *(Any other numbers that may be assigned this report)*
d.	N/A

10. DISTRIBUTION STATEMENT

[redacted]

11. SUPPLEMENTARY NOTES	12. SPONSORING MILITARY ACTIVITY
	U. S. Navy

13. ABSTRACT

The capture coefficients were determined for carbon dioxide, nitrogen, and argon on a flat cryopanel. The gas flow rates studied varied between 0.021 torr liters per second and 0.433 torr liters per second. For flow rates greater than 0.05 torr liters per second the capture coefficients for each of the gases decreased with an increasing flow rate. It was found that the capture coefficients of carbon dioxide also depend upon the cryopanel temperature. Above 0.05 torr liters per second the capture coefficients decreased with an increasing cryopanel temperature.

DD FORM 1 NOV 65 1473 (PAGE 1)

S/N 0101-807-6811

Unclassified

Security Classification

A-31408

14 KEY WORDS	LINK A		LINK B		LINK C	
	ROLE	WT	ROLE	WT	ROLE	WT
Capture Coefficient						
Cryogenic Pumping						
High Vacuum						